Feasibility Study for Gas-Grain Simulation Facility

J. B. Miller
B. C. Clark
Martin Marietta Astronautics Group
P.O. Box 179
Denver, Colorado 80201

**NASA**
National Aeronautics and
Space Administration

**Ames Research Center**
Moffett Field, California 94035

FOREWORD

---------------------------------------------------------------------------------

This final report, submitted to RCA Government Services in fulfillment of
contract G788563-J42, discusses the feasibility of a gas grain simulation
facility for the Space Station.

LIST OF TABLES

# LIST OF FIGURES

# 1.0   INTRODUCTION

This report discusses various physics aspects of gas/grain experiments
in microgravity.  Its primary purpose is to elucidate the problems that
must be dealt with and in many cases to assign values to the factors
involved.  This work is intended as a preliminary survey-type approach
and must be followed up in each individual specific experiment to
confirm the feasibility of the design.  The report is organized as
follows:

        (a)     forces on individual particles,
        (b)     levitation and particle handling methods,
        (c)     levitation induced coagulation forces,
        (d)     feasibility of long duration experiments,
        (e)     feasibility of classes of experiments, and
        (f)     summary and recommendations.

## 2.0 FORCES ON INDIVIDUAL PARTICLES

This section covers forces that act on individual particles. A later section covers the net effect of levitation-induced forces that tend to coagulate the particles.

## 2.1 INTERPARTICLE FORCES

Interparticle forces are due to Van der Waals attraction, electrostatic attraction, surface tension, and mutual shielding from the gas.

## 2.1.1 VAN DER WAALS FORCES

Van der Waals forces are defined as those that form the basis for the constant "a" in Van der Waals equation of state for a gas. They include forces between molecules having dipoles and quadrupoles, forces resulting from the polarization of molecules by static dipole or quadrupole fields of other molecules, and the nonpolar Van der Waals forces. Except when the dipole moment is large and the polarizability is small, the nonpolar forces (called dispersion forces) will be the largest (Corn, 1966).

The nonpolar Van der Waals forces between two particles depend on the electrodynamic properties of their respective media. Since there is a finite time of propagation of electromagnetic waves between the two particles, the effects are retarded and the potential is reduced (a very readable explanation of retarded potentials is given by Spruch, 1986). Modern Van der Waals theory was developed by Lifshitz (Marlow, 1980). For separation distance very much less than the wavelength of the interaction, Lifshitz theory reduces approximately to the (non-retarded) London Van der Waals dispersion forces as applied to condensed matter by Hamaker. Therefore for two spheres the attractive force for distance less than 1 nm is (Zimon, 1980)

$$F = \frac{A\, a_1\, a_2}{6\, d^2\, (a_1 + a_2)}, \qquad\qquad (2.1.1\text{-}1)$$

where

$A$   =   Hamaker constant for the interacting media (J),

$a_1, a_2$   =   radii of spheres (m), and

$d$   =   distance between surfaces (m).

For separation distances very much greater than the wavelength of the interaction (>50 nm), Lifshitz theory reduces to the (fully retarded) theory (Marlow, 1980). Therefore for large d (Zimon, 1980)

$$F = \frac{4 B a_1 a_2}{3 d^3 (a_1 + a_2)},$$

(2.1.1-2)

where B (J-m) is an interaction constant.

In aerosol microphysics, Van der Waals forces are important for particle separations less than a radius (Marlow, 1980). For $d \ll a$ (radius of smaller sphere), an approximate expression for the partially retarded interaction potential energy between two smooth spheres is (Gregory, 1981)

$$V = -\frac{A a_1 a_2}{6 d (a_1 + a_2)} \left[ 1 - \frac{bd}{\lambda} \ln \left( 1 + \frac{\lambda}{bd} \right) \right],$$

(2.1.1-3)

where

$\lambda$ = characteristic wavelength of the electromagnetic interaction $(\sim 10^{-7} m)$, and

$b \sim 5.32$ .

In Eq. 2.1.1-3 the term in brackets accounts for retardation. The Hamaker constant may be computed from dielectric data for the two particles and the gas (Hough and White, 1980). Some theoretically computed values of the Hamaker constant for particles in air are listed in Table 2.1.1-1. Some experimental values of the Hamaker constant for particles in a vacuum are $4.7 \times 10^{-19}$ J for borate and $2.2 \times 10^{-19}$ J for quartz (Corn, 1966).

For spherical particles with rough surfaces, the right hand side of Eq. 2.1.1-3 should be multiplied by the factor d/s, where d is now defined to be "the distance between outermost peaks of surface irregularities and s is the separation between the mean profile lines" (Czarnecki, 1984) (See Fig. 2.1.1-1).
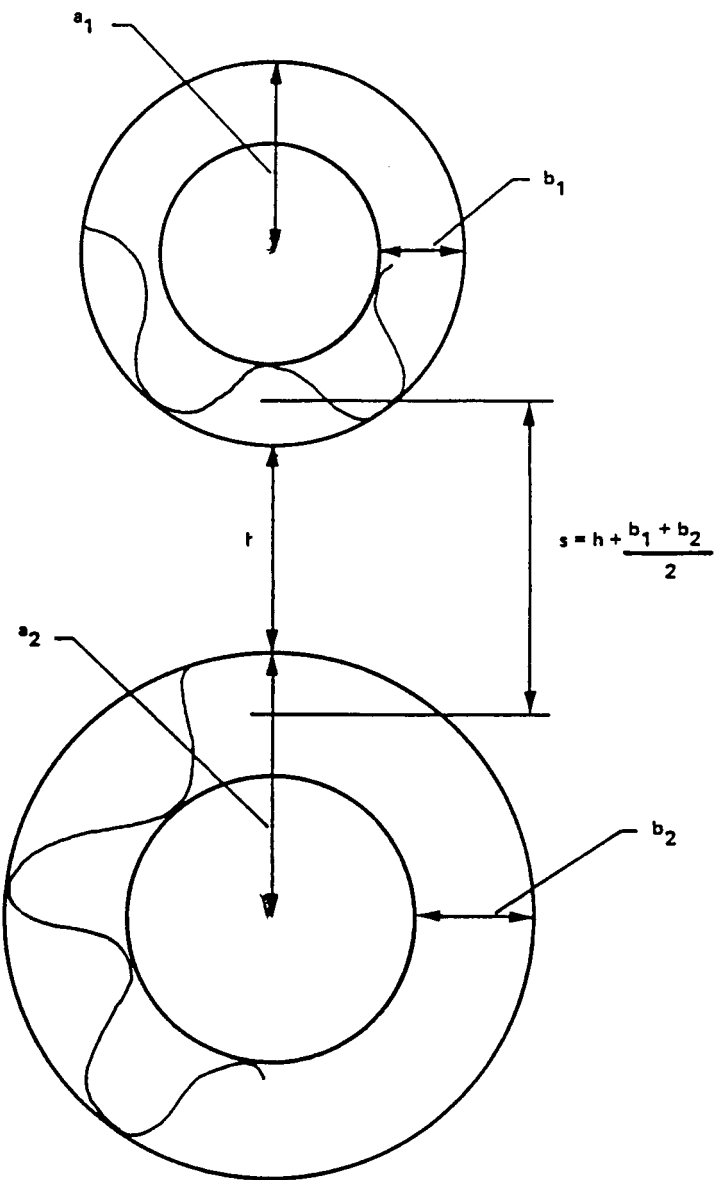
*Figure 2.1.1-1  Rough Spherical Particles*

For nonspherical particles such as flat plates, rectangular rods, and cylinders, particle orientation has an important effect on interparticle forces. These particles usually orient themselves such that the largest plane areas are opposed, which minimizes the potential energy (Hidy, 1984).

Even in a vacuum, the calculation of Van der Waals forces is at best approximate because of uncertainties in composition, size, shape, surface roughness, orientation, and spacing. In a gas, the dispersion force may be overwhelmed by adhesion forces due to electrostatic charge or absorbed molecules, in which case the dispersion force calculation is valuable only as an order of magnitude estimate (Corn, 1966).

Van der Waals forces scale with particle radius while gravitational forces scale with radius cubed. Thus Van der Wals forces become less important with increasing particle size (Corn, 1966).

Temperature affects Van der Waals forces. However, temperature effects that are confined to the oscillator modes of a particle may be neglected for $(hc/kT) \gg$ diameter where T is the particle temperature (Marlow, 1980).

Table 2.1.1-1    Theoretical Values of the Hamaker Constant for Particles in Air (from Hough and White, 1980).

| Material of Particle | Hamaker Constant $(\times 10^{-20} J)$ |
|---|---|
| Crystalline quartz | 8.83 |
| Fused quartz | 6.50 |
| Fused silica | 6.55 |
| Calcite | 10.1 |
| Calcium fluoride | 7.2 |
| Sapphire | 15.6 |
| Poly (methylmethacrylate) | 7.11 |
| Poly (vinylchloride) | 7.78 |
| Polystyrene [a] | 6.58 |
| Polystyrene [a] | 6.37 |
| Poly (isoprene) | 5.99 |
| Poly (tetrafluoroethylene) | 3.80 |
| "Teflon FEP" [b] | 2.75 |

[a]    variation in refractive index between sources
[b]    using infrared data for poly (tetrafluoroethylene)

## 2.1.2 ELECTROSTATIC INTERPARTICLE FORCES

Particles in a cloud will be charged.  Even if the cloud is not charged initially it will become charged by diffusion of ions present in the gas and by contact charging.  Contact charging is not due to friction but results from the making and breaking of contacts.  The cloud will contain both negatively and positively charged particles with the equilibrium charge distribution being approximately Gaussian.  The charges increase slightly less rapidly than the square of the particle diameter (Corn, 1966).

The initial charge on liquid droplets may be due to spray electrification.  At an interface between a gas and certain liquid substances, electric dipoles are created with positive polarity inward and negative outward.  When the surface is disrupted to form fine droplets, charged particles result (Corn, 1966).

The origin of initial charge on solid particles is not well understood.  It may be complicated by the effect of surface impurities, films of moisture, formation of Helmholtz double layers or by electrolytic effects.  Electrification can also be affected by the state of the surface and heat and mechanical stresses of the material.  Also, certain materials may transfer ions across surfaces after initial contact (Corn, 1966).

Contact potential differences may also arise due to the surface effects of dissimilar materials.  Their electrostatic binding force is proportional to the particle dimension to the two-thirds power (Barengoltz and Edgars, 1975).

There is much experimental evidence for the great importance of electrostatic forces in the adhesion of particles.  On the other hand crude calculations show that for the electrostatic forces to exceed the Van der Waals forces the charges would have to be much larger than observed and would have to be greatly concentrated near points of contact (Corn, 1966).

A more recent book (Hidy, 1984) does not quantitatively improve much on the above references to Corn.  Hidy concludes his section on this subject with a call for more study:" . . . future work on the fundamental nature of adhesion must incorporate studies of electrical interactions between solids, as well as intermolecular interactions." Hidy's only theoretical reference on this subject is Derjaguin and Smilga (1967), no references to which have appeared in the Science Citation Index since 1982.

A computerized search of the last 10 years of the IEEE (including Physics) Abstracts and the Aerospace Abstracts for the keywords ["electrostatic?" with "interparticle" with ("force?" or "attraction" or "coagulation")] yielded 20 references none of which is relevant to the above discussion.

## 2.1.3   SURFACE TENSION

For a wet or dirty surface, the capillary effects of surface films may produce an additional attractive force.  Capillary condensation causes a film of water to form between the particles.  For a relative humidity of 100% and for two equal sized spheres in contact, the adhesive force due to surface tension is

$$F \approx 2\pi R_p \sigma ,$$                                                (2.1.3-1)

where $R_p$ is the radius of the particles and $\sigma$ is the surface tension.  Eq. 2.1.3-1 has been verified by direct experimental measurement.  The force will be less for a lower relative humidity. The adhesion due to surface films may exceed that resulting from either intermolecular (Van der Waals) or electrical forces (Hidy, 1984).

## 2.1.4   MUTUAL SHIELDING FROM THE GAS

The Knudsen number is

$$Kn = \lambda_g / R_p ,$$                                                 (2.1.4-1)

where

   $\lambda_g$ = mean free path of the gas (m), and

   $R_p$ = particle radius (m).

Table 2.1.4-1 lists the mean free path of nitrogen at 20°C. As $Kn \longrightarrow 0$ continuum theory applies, whereas as $Kn \longrightarrow \infty$ the dynamics is characterized by individual gas molecules colliding with the particle (Hidy, 1984) and is called the free-molecular regime (Marlow, 1980).  For $1 \le Kn \le 10$ the particle is in the transition regime.  For two nearby particles in the transition regime, gas-particle collisions are less frequent between the particles and the particles experience an effective attractive force (Marlow, 1980).

Table 2.1.4-1 Mean Free Path of Nitrogen at 20°C
(from CRC, 1982)

| Pressure (mm Hg) | Mean Free Path (m) |
|---|---|
| 1 | $4.5 \times 10^{-5}$ |
| 0.1 | $4.5 \times 10^{-4}$ |
| 0.01 | $4.5 \times 10^{-3}$ |
| 0.001 | $4.5 \times 10^{-2}$ |

Note: 1 mm Hg = 1 torr = 1.33 millibar.

## 2.1.5  OTHER FACTORS

An external electric field has an immediate effect for example by producing aggregate threads of particles.  It may also have a lasting effect in that polarization of particles has been found to persist after the field was shut off.  Other factors influencing adhesion include (a) chemical and electrical properties of the materials, (b) surface contamination, nature of the particle surface contact (particle size, shape, roughness and state of aggregation), (c) temperature, and (d) time of contact (Corn, 1966).

## 2.2  DRAG FORCE

Particle motion through a gas may be characterized by the Reynolds number Re and the Knudsen number Kn.  The Reynolds number is

$$Re = \frac{\rho_g v_p R_p}{\mu_g},$$  (2.2-1)

where

$R_p$ = particle radius (m),
$v_p$ = particle velocity relative to gas (m/s),
$\rho_g$ = mass density of gas (kg/m$^3$), and
$\mu_g$ = viscosity of gas (kg/m-s).

The drag force acting on a particle is

$$F = \frac{v_p}{B},$$  (2.2-2)

where B is the mobility. For Kn $\to$ 0, Re $\ll 1$, the mobility of a spherical particle is

$$B = \frac{1}{6 \pi \mu_g R_p},$$

(2.2-3)

For $K_n \to 0$, Re $\leq 1$,

$$F = \frac{1}{2} \rho_g \pi R_p^2 C v_p^2, \text{ and}$$

(2.2-4)

$$C = (12/\text{Re})(1 + 0.250 \text{ Re}^{2/3}).$$

(2.2-5)

For $K_n \neq 0$, Re $< 1$,

$$B = \frac{A}{6 \pi \mu_g R_p}, \text{ and}$$

(2.2-6)

$$A = 1 + 1.257 \text{ Kn} + 0.400 \text{ Kn exp} (-1.10 \text{ Kn}^{-1}).$$

(2.2-7)

Nonspherical particles are included by use of dynamic shape factors (Hidy, 1984).

## 2.3    BROWNIAN MOTION

The mean square displacement of a particle due to Brownian motion is (Spurny, 1986)

$$\Delta x^2 = 2 t k T B,$$

(2.3-1)

where

t = time(s),

k = Boltzmann constant $(1.3804 \times 10^{-23}$ J/K),

T = gas temperature (K), and

B = mobility of the particle.

10

The number of particles striking the entire inner surface per unit time of a sphere of radius a is (Hidy, 1984)

$$8a \, \pi D_p \, N_\infty \sum_{n=1}^{\infty} \exp \left( \frac{-n^2 \, \pi^2 \, D_p \, t}{a^2} \right) , \qquad (2.3\text{-}2)$$

where

$N_\infty$ = initial particle concentration far from the wall, and

$D_p$ = BkT.

It is useful to compare Brownian motion with that due to the terminal velocity at $10^{-5}$ g. The particle is placed at the center of a spherical chamber of radius x. At terminal velocity the drag force of Eq. 2.2-2 equals $m(10^{-5}$ g). Assuming that the terminal velocity is reached instantaneously, the time until the particle hits the spherical wall is

$$t_g = \frac{9 \, \mu_g \, x}{2R_p^2 \, \rho_p \, A \, (10^{-5} \, g)} , \qquad (2.3\text{-}3)$$

where $\rho_p$ is the mass density of the particle and A is given by Eq. 2.2-7. The time for the particle to reach the wall by Brownian motion is

$$t_B = \frac{3 \, \pi \, \mu_g \, R_p \, x^2}{k \, T \, A} . \qquad (2.3\text{-}4)$$

For a chamber of radius 0.5 m, for nitrogen gas at 300 K, and for particles of mass density 1 gm/cm$^3$, particle radii corresponding to various values of $t_B/t_g$ are listed in Table 2.3-1. For a chamber of radius 0.5 m, nitrogen gas at 300 K, and a particle of mass density 1 gm/cm$^3$, these times are evaluated for various particle radii and gas pressures in Tables 2.3-2 and 2.3-3. From Table 2.3-2 it may be noted that at a pressure of 1 mm Hg, Brownian motion causes a particle of radius 1 nm to reach the wall in only two minutes. In particular, the nanometer sized grains that are nucleated at a pressure of 0.2 mb (0.15 mm Hg) in the Titan aerosol experiment (McKay et al., 1986) would reach the wall by Brownian motion in 20 seconds [if they were not formed in some kind of levitation well and if they did not first coagulate (coagulation depends on particle number density, which was not specified)].

Table 2.3-1 Radii for Various Ratios of Times, until Particle Hits Wall
by Brownian Motion and $10^{-5}$g.

| $t_B/t_g$ | $R_p$(μm) |
|-----------|-----------|
| 0.1       | 0.16      |
| 1         | 0.34      |
| 10        | 0.74      |

Conditions:
$T$ = 300 K
$\rho_p$ = 1 g/cm$^3$
$x$ = 0.5 m

Table 2.3-2 Time Until Particle Hits Wall
          Due to $10^{-5}$g and Brownian Motion
          (Gas Pressure = 760 mm Hg)

| $R_p$(m) | Kn | A | time (s) $10^{-5}$g | Brownian |
|---|---|---|---|---|
| $10^{-9}$ | 59 | 98 | $4.2 \times 10^{12}$ | $1.0 \times 10^5$ |
| $10^{-8}$ | 5.9 | 10 | $4.1 \times 10^{11}$ | $1.0 \times 10^7$ |
| $10^{-7}$ | 0.59 | 1.8 | $2.3 \times 10^{10}$ | $5.6 \times 10^8$ |
| $10^{-6}$ | 0.059 | 1.1 | $3.7 \times 10^8$ | $9.2 \times 10^9$ |
| $10^{-5}$ | 0.0059 | 1.0 | $4.1 \times 10^6$ | $1.0 \times 10^{11}$ |
| $10^{-4}$ | $5.9 \times 10^{-4}$ | 1.0 | $4.1 \times 10^4$ | $1.0 \times 10^{12}$ |
| $10^{-3}$ | $5.9 \times 10^{-5}$ | 1.0 | $4.1 \times 10^2$ | $1.0 \times 10^{13}$ |

Conditions:
    Chamber radius:      0.5 m
    Gas:                 Nitrogen
    Temperature:         300 K
    Particle density:    1 g/cm$^3$

Table 2.3-3 Time Until Particle Hits Wall
          Due to $10^{-5}g$ and Brownian Motion
          (Gas Pressure = 1 mm Hg)

| $R_p$(m) | Kn | A | time (s) $10^{-5}g$ | Brownian |
|---|---|---|---|---|
| $10^{-9}$ | $4.5 \times 10^4$ | $7.5 \times 10^4$ | $5.4 \times 10^9$ | $1.4 \times 10^2$ |
| $10^{-8}$ | $4.5 \times 10^3$ | $7.5 \times 10^3$ | $5.4 \times 10^8$ | $1.4 \times 10^4$ |
| $10^{-7}$ | $4.5 \times 10^2$ | $7.5 \times 10^2$ | $5.4 \times 10^7$ | $1.4 \times 10^6$ |
| $10^{-6}$ | 45 | 75 | $5.4 \times 10^6$ | $1.4 \times 10^8$ |
| $10^{-5}$ | 4.5 | 8.1 | $5.0 \times 10^5$ | $1.2 \times 10^{10}$ |
| $10^{-4}$ | 0.45 | 1.6 | $2.6 \times 10^4$ | $6.3 \times 10^{11}$ |
| $10^{-3}$ | 0.045 | 1.1 | $3.7 \times 10^2$ | $9.2 \times 10^{12}$ |

Conditions:
    Chamber radius:    0.5 m
    Gas:               Nitrogen
    Temperature:       300 K
    Particle density:  1 g/cm$^3$

## 2.4   EXTERNAL QUASISTATIC FIELDS

The force due to external fields is

$$\vec{F} = m_p \vec{g} + q_p (\vec{E} + \vec{v}_p \times \vec{B}),$$  (2.4-1)

where

$m_p$  = mass of the particle (kg),

$\vec{g}$  = acceleration of gravity (m/s$^2$),

$q_p$  = charge on the particle (C),

$\vec{E}$  = electric field (V/m),

$\vec{v}_p$  = particle velocity (m/s), and

$\vec{B}$  = magnetic field (T).

## 2.5    ALTERNATING MAGNETIC FIELD

An alternating magnetic field will generate eddy currents in a spherical particle. The eddy currents will be strongest at the surface. By Lenz's law, the currents will act to oppose the field and tend to exclude it from the inside of the particle. For a field $B_O$ that varies slowly in the axial direction, the axial force is

$$F = \frac{-\pi a^3}{\mu_o} \nabla B_o^2 , \qquad (2.5-1)$$

where a is the radius of the particle (Frost and Change, 1982).

## 2.6    G-JITTER

Random accelerations that affect a particle are called g-jitter and are due to crew motion, docking, equipment operation, etc. They may be approximated by a time varying acceleration (McKay et al., 1986)

$$a_r = a_o \sin(\omega t), \qquad (2.6-1)$$

where

$a_O$ = amplitude of the acceleration ($m/s^2$), and

$\omega$ = angular frequency ($s^{-1}$).

For $Kn \rightarrow \infty$ and the maximum displacement $X_0 \ll \lambda_g$, it is called ballistic g-jitter and the particle behaves as if it were in a vacuum. For $X_0 \gg \lambda_g$ drag forces must be considered: for $Kn \rightarrow \infty$ it is called Knudsen g-jitter and for $Kn \rightarrow 0$ it is called Stokes g-jitter (McKay et al., 1986).

## 2.7    PHORESIS

If an aerosol particle is in a temperature gradiant, light, or vapor-concentration gradient, the Brownian motion is biased toward one direction and this is called a phoresis. Thermophoresis, photophoresis, and diffusiophoresis will occur, respectively (Spurny, 1986).

## 2.7.1 THERMOPHORESIS

The force due to a temperature gradient on a spherical particle is
(Hidy, 1984)

$$\vec{F} = - \frac{32}{15} R_p^2 \frac{k_g}{\overline{v}_g} \nabla T \exp\left(\frac{\hat{\tau} R_p}{\lambda_g}\right), \qquad (2.7.1\text{-}1)$$

for $0.25 \leq \lambda_g/R_p \leq \infty$, $Ma \ll 1$,

where

$\overline{v}_g$ = mean thermal speed of the gas (m/s),

$\lambda_g$ = mean free path of the gas (m),

$M_a$ = Mach number,

$$M_a = v_p / \overline{v}_g, \qquad (2.7.1\text{-}2)$$

$$\hat{\tau} = 0.9 + 0.12 \, \alpha_m + 0.21 \, \alpha_m \left(1 - \frac{\alpha_t \, k_g}{2 \, k_p}\right) \qquad (2.7.1\text{-}3)$$

(for monatomic gases),

$\alpha_m$ = accommodation coefficient for momentum,

$\alpha_t$ = accommodation coefficient for heating,

$k_g$ = thermal conductivity of the gas (J/m-s-K), and

$k_p$ = thermal conductivity of the particle (J/m-s-K).

The accommodation coefficients vary from zero to unity and must be
measured for each material combination (Hidy, 1984).

## 2.7.2 PHOTOPHORESIS

Photophoresis is due to heating of the particle on one side by light. The gas on that side is heated and the particle moves in the opposite direction. In positive photophoresis, the particle moves in the same direction as the light, while in negative photophoresis it moves toward the light source (Preining, 1966).

In a beam of light, a sphere may form a lens, causing the light to be refracted within the particle. There are two cases. For a weakly absorbing particle, the image of the light source is close to the dark side of the particle. A small weakly absorbing particle will be heated more on the dark side and will exhibit negative photophoresis, while a large particle (due to absorption) will be heated more on the lighted side and will exhibit positive photophoresis. A strongly absorbing particle will be heated more on the lighted side and will always exhibit positive photophoresis (Preining, 1966).

Negative photophoresis may be observed by shining laser light on smoke particles (which are not totally opaque) in air (Ashkin, 1972).

## 2.7.3 DIFFUSIOPHORESIS

The diffusion force depends on the concentrations, gradients, molecular masses, and diffusion coefficients of the gas species involved and also on the cross section of the particle (Hidy, 1984).

## 2.8 RADIATION PRESSURE

Light carries momentum and thus exerts force on a particle when it is reflected, refracted, or absorbed by it. The momentum carried by a photon is

$$p = \frac{E}{c},$$  (2.8-1)

where

E = energy of the photon (J), and

c = speed of light ($2.998 \times 10^8$ m/s).

An absorbed photon imparts all of its momentum to the particle. A photon elastically scattered by 180° imparts twice its momentum to the particle. A photon refracted or reflected at some other angle imparts momentum according to the laws of conservation of energy and momentum. For a light intensity gradient perpendicular to the direction of the light, a component of force is applied perpendicular to the direction of light. For highly reflective particles, the force is toward the region of lesser intensity. For transparent particles with index of refraction greater than that of the surrounding media, the force is toward the region of greater intensity (Ashkin, 1972).

2.9    ACOUSTIC FORCE

A standing sound wave produces through a nonlinear effect an average ambient pressure change of (Wang, 1986)

$$<\Delta p> \ = \ \frac{\overline{p^2}}{2\rho c^2} \ - \ \frac{\rho \, \overline{u^2}}{2} \, , \tag{2.9-1}$$

where

$\overline{p^2}$ = time average of square of instantaneous pressure (Pa$^2$),

$\rho$ = mass density of gas (kg/m$^3$),

c = speed of sound in gas (m/s), and

$\overline{u^2}$ = time average of square of instantaneous gas velocity (m$^2$/s$^2$).

When placed in a standing wave field, a sphere experiences a radiation pressure force of (Wang, 1986)

$$F \ = \ \left(\frac{5\pi}{6}\right) \left(\frac{p_1^2}{\rho c^2}\right) \ k \, a^3 \sin 2kx \, , \tag{2.9-2}$$

where

$p_1$= pressure amplitude of the fundamental frequency (Pa),

k = wave number ($m^{-1}$),

a = sphere radius (m), and

x = position of center of sphere (m).

Eq. 2.9-2 is the basis of acoustic levitation and has the following limitations:

(a) the mass density of the sphere must exceed that of the gas;

(b) the diameter of the sphere must be much less than the wavelength; and

(c) the diameter of the sphere must be greater than the mean free path of the gas (McKay et al., 1986).

It is obvious from Table 2.1.4-1 that acoustic levitation can not confine a nanometer sized particle that first nucleates from a few molecules of the product of a gaseous chemical reaction. Also, Appendix C shows that for frequencies very much less than MHz, acoustic levitation prevents Brownian motion of the levitated particle.

It should be noted that the force given by Eg. 2.9-1 is proportional to the volume. The sphere also experiences the viscous drag force of acoustic streaming, which depends on the surface area of the sphere and is a complicated function of (a) the geometry of the transducer, (b) the schemes for the production of standing waves, and (c) the acoustic boundaries (Lee and Feng, 1982). The levitation becomes unstable when the streaming force becomes as high as 25% - 75% of the volumetric force. As the size of the particle is decreased, the ratio of the streaming force to the volumetric force increases. However the ratio may be reduced by using a higher frequency (Lee and Feng, 1982) (see Fig. 2.9-1). M. Barmatz of JPL (private communication via G. Fogleman of RCA, July, 1987) has estimated that streaming limits the minimum particle radius to 1% of the wavelength.
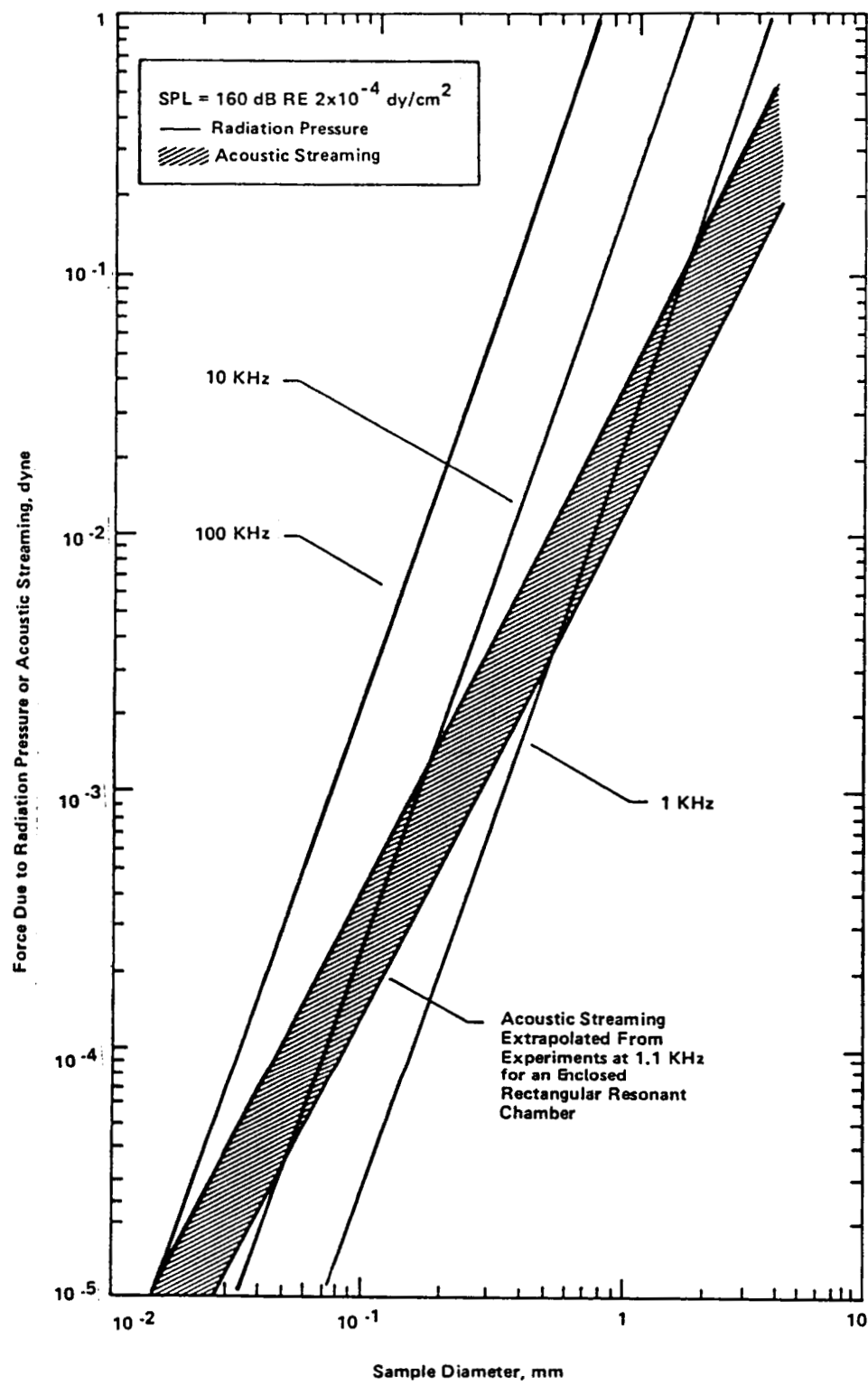
Figure 2.9-1 Force of Radiation Pressure or Acoustic Streaming (Lee and Feng, 1982)

21

3.0    LEVITATION AND PARTICLE HANDLING METHODS

The levitation methods considered are

    (a)   none (chemically inactive walls),
    (b)   light pressure,
    (c)   radiometric,
    (d)   acoustic,
    (e)   electrostatic,
    (f)   aerodynamic, and
    (g)   electromagnetic.

3.1    NO LEVITATION

Many cloud type experiments do not require levitation but should use
inert walls.  This would avoid the artificial coagulation caused by all
of the levitation methods.  Many walled cloud experiments that are
currently performed on Earth would be much better in space because
particles could grow to much greater size before they precipitated due
to the residual gravity.

3.2    LEVITATION BY LIGHT PRESSURE

Levitation by light pressure is possible for highly transparent
particles and for highly reflective particles (Ashkin, 1972).
Partially transparent (absorptive) particles would be heated to the
point where melting or chemical changes would have to be considered and
in a gas would be subject primarily to radiometric (photophoretic)
forces.  Highly reflective particles [reflectivity >> 98% (Ashkin,
1972)] would not correspond to the cases of interest.  Therefore the
following will be restricted to highly transparent particles.

In a microgravity environment two opposing beams would be used (see
Fig. 3.2-1).  The index of refraction of the particle is greater than
that of the gas.  The laser beam has a Gaussian intensity distribution,
which causes the centering of a particle in the beam.  The particle is
also pushed with the beam, and the diffusive spreading of the
oppositely directed beams produces a trap for the particle (Ashkin,
1972).

For sufficient gas pressure, the fluid damping (Ashkin, 1972) would be
sufficient for stable confinement of many particles simultaneously.  In
a vacuum, active feedback of laser power might have to be used and thus
confinement might be restricted to one particle.
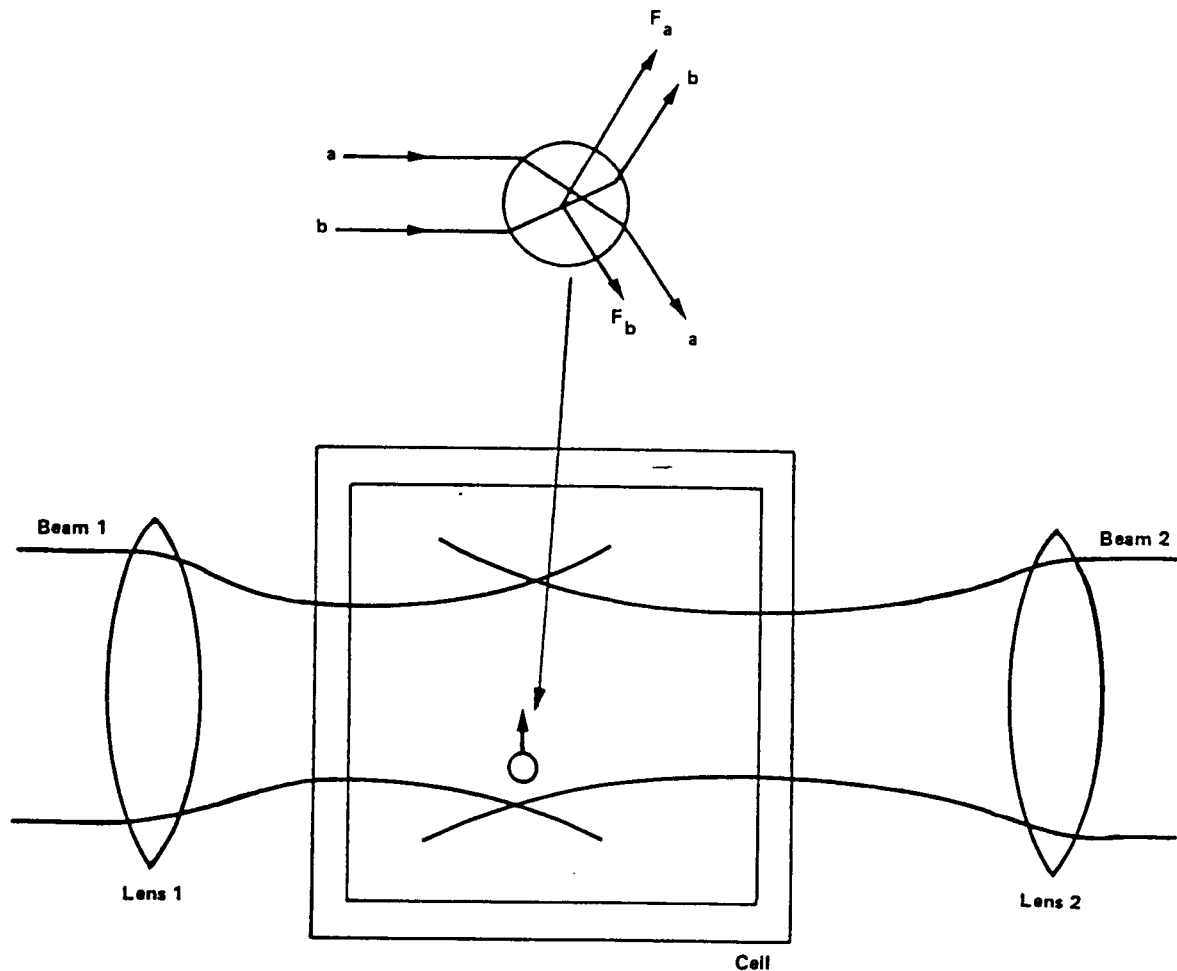
*Figure 3.2-1*
*Optical Bottle Refraction for Centering Small Transparent Particles (Ashkin, 1972)*

It is possible to confine nonspherical particles. However, they become oriented in the beam (Ashkin and Dziedzic, 1980) and this would prevent a realistic study of coagulation processes.

It is also possible to achieve stable confinement by an alternating light trap (Ashkin and Dziedzic, 1985). However, this would not have any advantages and would require many more optical components. Another method is to use the strong light gradient forces at a single optical focus (Ashkin et al., 1986). However, this restricts the trap to a very small size and would thereby preclude multiple particle experiments.

A small number of particles (2-20) might be confined by directed pulses of laser light.

## 3.3 RADIOMETRIC LEVITATION

For highly absorbing particles in a gas, the radiometric (photophoretic) forces greatly exceed those due to light pressure (Lewittes and Arnold, 1982). A stable trap has been demonstrated in which a TEM01* (doughnut) mode laser shines upward and suspends highly absorbing particles against the force of gravity. The TEM01* mode has an intensity minimum at the center and thus highly absorbing particles are confined both radially and vertically (see Fig. 3.3-1) (Lewittes and Arnold, 1982). It seems reasonable that two opposing TEM01* lasers could create a stable trap in microgravity (see Fig. 3.3-2). This would certainly be true if feedback control of laser power were used to confine a single particle. However, even without feedback a cloud of particles could probably be confined.

The situation with less highly absorbing particles is more complicated and depends on their size and the gas pressure. Small particles will be subject to negative photophoresis and will move toward the light source [but also perpendicular to the light in the direction of an intensity minimum (Lewittes and Arnold, 1982)]. A single small particle could be confined by applying feedback to the configuration of Fig. 3.3-2 (a laser's intensity would be increased to attract the particle toward it). There does not appear to be a way of confining a cloud of particles small enough to be subject to negative photophoresis. Also, for weak enough absorption and a very high or low gas pressure, the light pressure forces may predominate over the radiometric forces. This is because the radiometric force is maximized at the pressure at which the mean free path of the gas is equal to the diameter of the particle (Ashkin and Dziedzic, 1976).
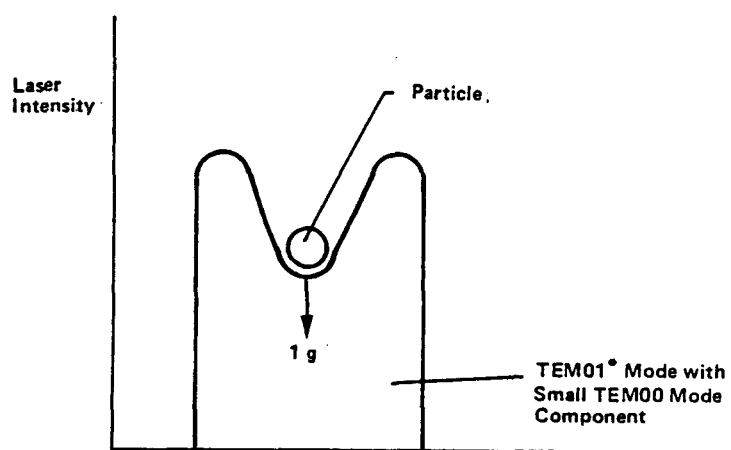
*Figure 3.3-1*
*Radiometric Levitation of Highly Absorbing Particle at 1 g*
*(Lewittes and Arnold, 1982)*
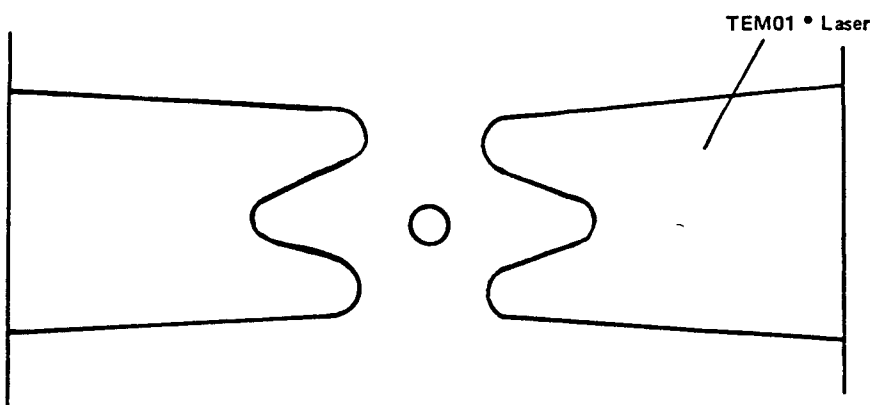
*Figure 3.3-2*
*Radiometric Trap for Highly Absorbing Particles in Microgravity*

Larger and less highly absorbing particles are subject to positive
photophoresis and would behave similarly to the highly absorbing
particles described above. This would be true if all particles were
greater than a certain critical size. However, it does not seem
possible to confine a cloud of small particles (subject to negative
photophoresis) and then continue to confine them as some grow to sizes
subject to positive photophoresis. This is particularly true since as
the size of a given particle reaches that at which positive and
negative photophoresis cancel the predominate radial force would be
that of light pressure, which would force the particle to the outside
of the TEM01* laser beam. This effect may preclude radiometric
confinement during nucleation and growth of even a single particle,
although perhaps a careful procedure may circumvent this for a single
particle.

## 3.4    ACOUSTIC LEVITATION

The acoustic approach is one of the most highly developed types for
levitation in microgravity and on Earth. Here, the emphasis will be on
the leading types of acoustic levitation for microgravity: single-axis
interference and tri-axis. However, other types will be mentioned
because they may fill special needs.

### 3.4.1    SINGLE AXIS ACOUSTIC INTERFERENCE LEVITATION

In single axis interference levitation, a small reflector
(diameter $\approx \lambda$  .= sound wavelength) is placed an arbitrary distance
from a fixed frequency ultrasonic source. The reflected sound wave
interferes with the incident sound wave to produce a region of minimum
acoustic potential energy at a distance of slightly more than $\lambda/4$ from
the reflector (see Fig. 3.4.1-1) (Day and Ray, 1986). This potential
well, which is deep in the axial direction and shallow in the radial
direction, traps the particle (Day and Ray, 1986). The reflector and
driver are made slightly convex to focus the sound (Naumann and
Elleman, 1986).

The walls of the chamber are designed to absorb sound (Naumann and
Elleman, 1986) and plane surfaces are avoided (Whymark et al., 1979).
Careful choice of chamber dimensions avoids resonances (Naumann and
Elleman, 1986). The gas absorption is selected carefully: if it is
too high, the energy well will be too weak; if it is too low,
reflections may be a problem (Whymark et al., 1979).
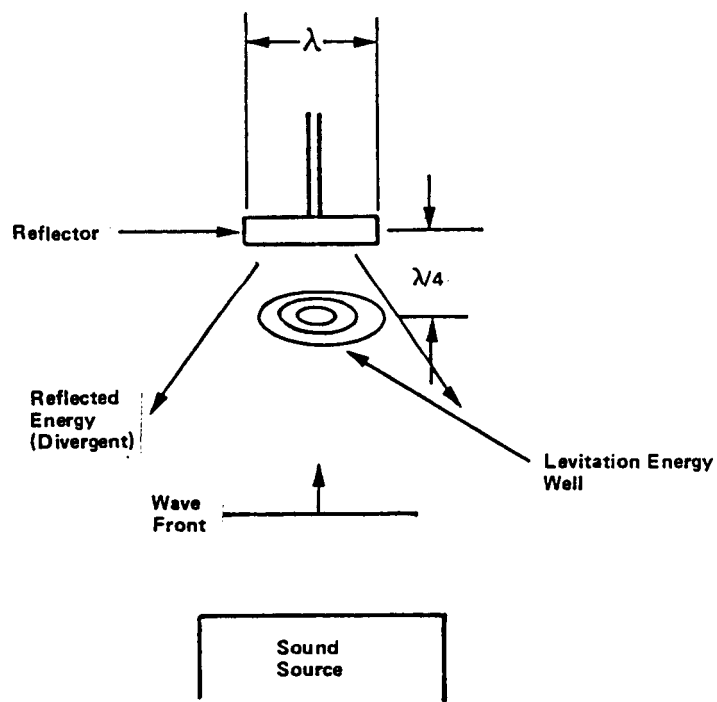
*Figure 3.4.1-1*
*Single-Axis Interference Acoustic Levitator (Day and Ray, 1986)*

There are a number of advantages with this technique. First, no tuned cavity is involved. Therefore as the gas density, composition, temperature, or the sample size changes, the equilibrium position simply moves slightly relative to the reflector (Naumann and Elleman, 1986). High specimen cooling rates (30°C/s) are possible (Day and Ray, 1986). Levitation has been demonstrated up to 1600°C (Whymark et al., 1979), although the levitation force diminishes approximately as the inverse 5/2 power of temperature (Naumann and Elleman, 1986).

Another advantage is that the sample may be moved by moving the reflector. In fact, multiple samples may be manipulated by the use of multiple reflectors (see Fig. 3.4.1-2 (a)). Liquid drops may be merged by tilting the reflectors until the potential wells overlap (see Fig. 3.4.1-2 (b)) (Whymark et al., 1979). Access is good from all sides except that of the sound source.

The primary disadvantage is the shallowness of the potential well in the radial direction. The radial restoring force is provided by the weak effect of the gas streaming past the sample (Bernoulli effect) (Naumann and Elleman, 1986). A sample that is well confined axially might be lost due to the transverse acceleration caused by astronaut motion. An associated disadvantage is that a liquid sample will not have a precisely spherical shape because the equipotential surfaces of the well are not spherical. In fact, large droplets of liquid having low surface tension (such as water) are broken up (Naumann and Elleman, 1986). Also, there is no independent control over sample rotation.

## 3.4.2 TRI-AXIS ACOUSTIC LEVITATION

The tri-axis levitator is comprised of three perpendicular sound sources and a cavity which is tuned for the fundamental mode for each of three perpendicular directions (see Fig. 3.4.2-1) (Barmatz, 1982). The sample is positioned at the middle of the cavity (Barmatz, 1982). By using a rectangular chamber with a square cross section and by maintaining a 90° phase difference between the driver located on the equal sides, the sample can be rotated. Vibrations can be induced in a liquid drop by causing a sinusoidal amplitude modulation in one of the drivers (Wang, 1983).

The primary advantage of the tri-axis levitator is that the acoustic well has spherical equipotential surfaces thus trapping the sample equally strongly from all directions and causing a liquid sample to remain spherical (Naumann and Elleman, 1986).

A disadvantage is that a change in gas temperature (Naumann and Elleman, 1986), composition or density requires adjustment of the frequency. Although changes in sample size also require frequency adjustment (Barmatz et al., 1983), the sample sizes of interest in gas-grain simulations will in most cases be too small to have any effect.

Reflectors

Samples

Sound Source

(a)

Reflectors

Liquid Samples Merging

Sound Source
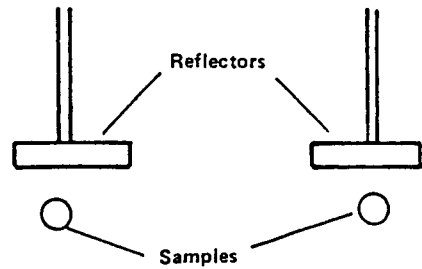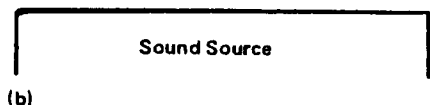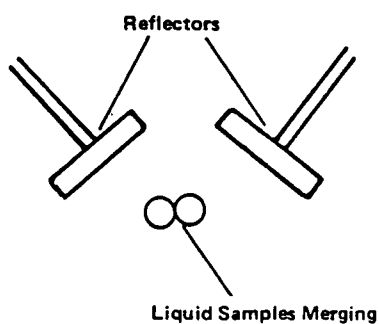
(b)

*Figure 3.4.1-2*
*Sample Manipulation Using Multiple Reflectors*
*(Whymark, et al., 1986)*
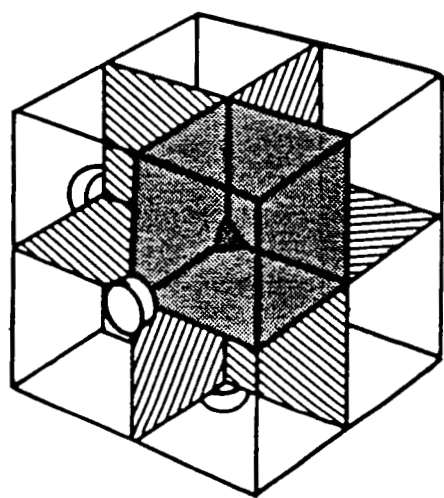
*Figure 3.4.2-1  Triple-Axis Acoustic Levitator (Barmatz, 1982)*

Another disadvantage is that only one sample can be levitated at a time. While the cavity walls may be constructed of plexiglass to enable visual inspection (Wang, 1986), the walls restrict mechanical access. Also, the gas temperature of the tri-axis system is currently limited to ∿ 600°C (Day and Ray, 1986). A limitation on the rate of temperature decrease (at constant position) to a few degrees per minute (Naumann and Elleman, 1986) would probably not affect most gas-grain experiments.

3.4.3   OTHER CONFIGURATIONS FOR ACOUSTIC LEVITATION

Some other configurations are the following:

(a) hemispherical focusing radiator,
(b) siren,
(c) tetrahedral arrangement of sound sources,
(d) ring-type radiator, and
(e) single-mode levitator.

Items (a), (b) and (e) were designed for use in 1 g, but might be useful for microgravity.

The hemispherical focusing radiator uses a spherical concave reflector placed one half of a wavelength beyond the focus of the radiator. The back surface of the radiator is covered with 130 piezo-electric transducers. The advantage of this configuration is that it concentrates a large sound power in a small area. Samples of submillimeter size have been levitated. One disadvantage is that it causes the sample to rotate (Lee and Feng, 1982).

The siren was designed to levitate large objects on Earth (Gammel et al., 1982). Its high power is not necessary for the levitation of small grains in microgravity and may cause noise pollution on the Space Station.

The tetrahedral arrangement of sources does not require any reflectors, but still offers somewhat limited access (see Fig. 3.4.3-1) (Hatano et al., 1982).

The focused ring source was designed to produce easy access around the object by using a single radiator (see Fig. 3.4.3-2). A piezoelectric - ceramic transducer drives the ring-type radiator through a solid horn. The ring is uniformly vibrated in the radial direction. Since the inside of the ring is tapered at an angle of 20°, the sound is focused a short distance from the ring (Hatano et al., 1982).

The single-mode acoustic levitator uses a single non-planar mode generated from a single transducer. It uses reflections from all of the walls and an adjustable plunger controls the chamber length (see Fig. 3.4.3-3). The "inherent phase coherence of the orthogonal force components automatically assures . . . " translational and rotational stability. By exciting more than one mode the sample can be rotated in a controlled manner (Barmatz, 1987).
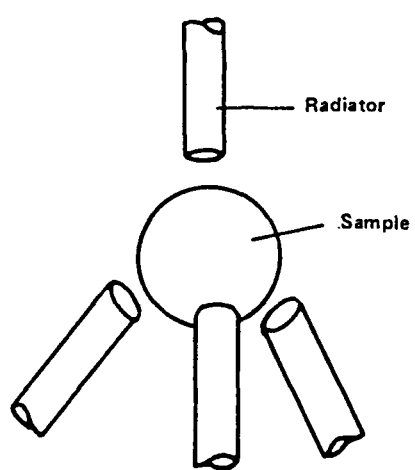
*Figure 3.4.3-1*
*Tetrahedral Arrangement of Sound Sources*
*(Hatano, et al., 1982)*
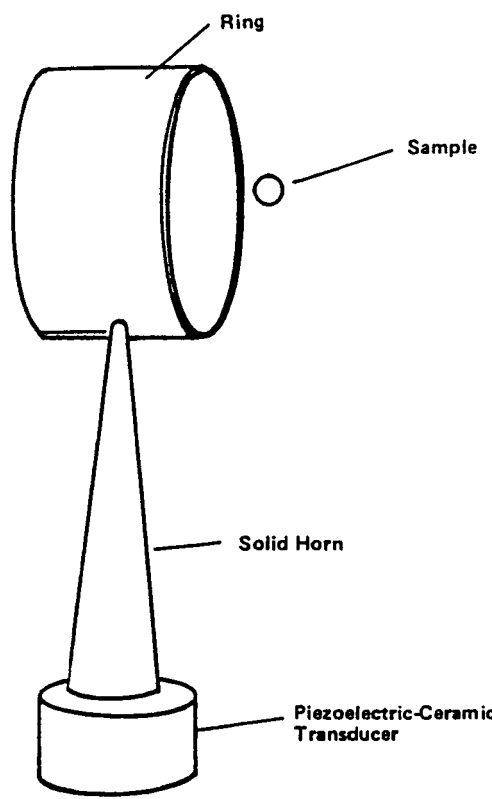
*Figure 3.4.3-2  Ring-Type Radiator (Hatano, et al., 1982)*

Adjustable
Plunger

Sample

Cylindrical
Chamber

Alumina
Rod

Horn of
Exponential
Shape

Piezoelectric
Transducer
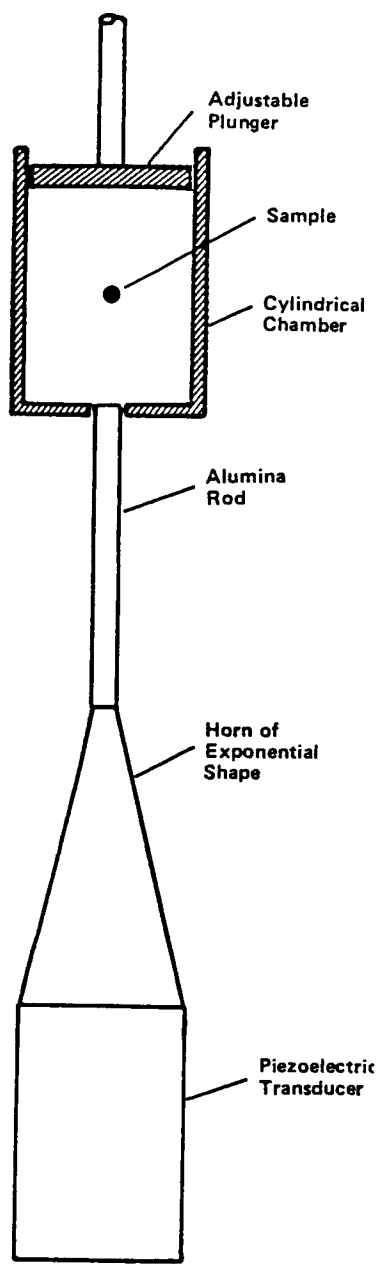
*Figure 3.4.3-3 Single - Mode Levitator (Barmatz, 1987)*

## 3.5    ELECTROSTATIC LEVITATION

Ernshaw's theorem states that stable confinement with static electric
fields is impossible (Rhim et al., 1985).  Therefore, it is necessary
to use either a feedback system or alternating electric fields.

Electrostatic levitation with feedback will work for particles of any
size and has been demonstrated in microgravity.  Levitation with
alternating electric fields has been demonstrated with small particles
in 1 g and may work in microgravity.

Electrostatic levitation works in a gas or vacuum with liquid or solid
particles that are conducting or nonconducting.

A dielectric particle having no net charge may be levitated in a
nonuniform electric field.  Appendix B shows that this is probably
infeasible for gas-grain applications.

### 3.5.1    ELECTROSTATIC LEVITATION WITH FEEDBACK

The best electrostatic levitation method for large objects appears to
be the tetrahedral positioner, in which spherical electrodes are
located at the verticles of a tetrahedron (see Fig. 3.5.1-1).  Two
cameras sense the position of the object and a proportional-
integral-differential feedback algorithm is used to center it.  The
advantage of the tetrahedral positioner over the single-axis (eg.
ring-type with feedback) positioner is that the damping (derivative
term) is applied to oscillations in all directions.  Since the
development of the tetrahedral positioner emphasized application to
materials processing, any problems with application to very small
particles were not detailed.  (Rhim et al., 1985).

Initial charging of a (solid) object to be levitated may be by contact
with one of the electrodes.  For levitation for long periods and
especially at high temperatures, additional charging may be provided by
a pulse-charging system (Makin et al., 1986).

### 3.5.2    LEVITATION WITH ALTERNATING ELECTRIC FIELDS

A very convenient method for levitating and studying an aerosol
particle in 1 g is through the combination of static and alternating
electric fields shown in Fig. 3.5.2-1.  The static voltage $V_{dc}$
balances gravity.  For a sufficiently high frequency, alternating
voltage applied to the central ring the particle will remain
stationary.  No feedback system is required (Straubel and Straubel,
1986).  The reference did not make clear if the particle would remain
stationary in microgravity with $V_{dc} = 0$.

## 3.6    AERODYNAMIC LEVITATION

The following types of aerodynamic levitation are orientation-
independent and therefore may be used in microgravity:
constricted-tube gas-flow, triaxial sonic pump, and triaxial molecular
beam.  Plasma levitation may also be configured for microgravity.
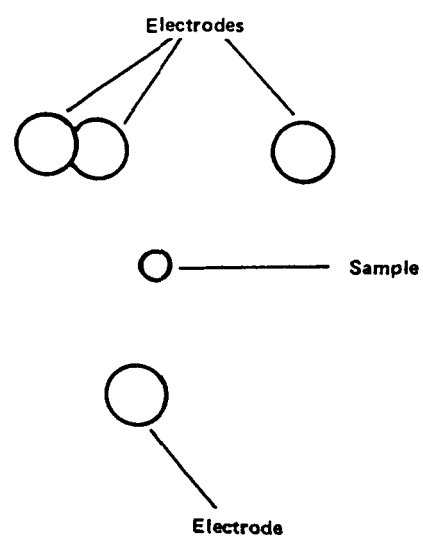
*Figure 3.5.1-1  Tetrahedral Electrostatic Positioner*
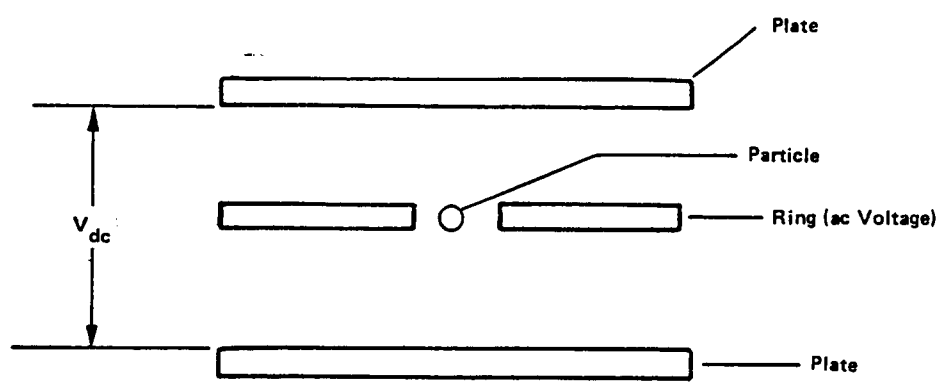
*Figure 3.5.2-1  Levitation with Static and Alternating Electric Fields*

### 3.6.1  CONSTRICTED-TUBE GAS-FLOW LEVITATION

The tube contains identical converging and diverging regions on the upstream and downstream ends of the constriction (see Fig. 3.6.1-1). The pressure and flow are adjusted such that the sample is held at the downstream end of the constriction.  A suction source is placed downstream.  A uniform velocity distribution upstream and turbulent free flow throughout is provided by antivortex screens in a stilling chamber upstream of the constriction.  The flow rate is controlled by vanes in the upstream volume (Berge et al., 1981) (Rush, 1981).

An advantage of this levitator is that feedback is not required. Disadvantages are that the sample is caused to rotate and that a solid sample must be spherical (Rush, 1981).  Another disadvantage is that the flow may affect the reaction rate (eg. chemical reaction, adsorption, etc.) in a gas grain experiment.

### 3.6.2  TRIAXIAL SONIC PUMP LEVITATION

A sonic pump is a loudspeaker driven device that produces a directed flow of gas.  Six of these may be directed inward in opposing pairs along three orthogonal axes and combined with an electro-optical detection and feedback system to produce a levitation system.  A sonic pump is simply a speaker connected to a tube (see Fig. 3.6.2-1). During one half cycle of the speaker cone, gas enters the tube isotropically.  During the other half cycle gas leaves the tube with directed flow outward.  The pulsed nature of the outward flow is detectable for only a short distance beyond the end of the tube.  The levitated object, which is many tube diameters away, experiences a steady flow.  The advantage of the sonic pump is that it can control gas flow with shorter response time than could any mechanical valve (Dunn, 1985).

Sonic pump closures with single orifices are used to levitate large spheres, while multiple orifice closures (collimated hole structures) are used for smaller objects (Dunn, 1985).

An advantage of this system is that is it not dependent upon temperature (Dunn, 1985).

### 3.6.3  TRIAXIAL MOLECULAR BEAM LEVITATION

For levitation at very low pressures molecular beams may be arranged in a triaxial configuration and a vacuum pump may be applied to the levitation chamber.  Each molecular beam may emanate from a single capillary or a collimated hole structure may be used.  Because of electrostatic charging and polarization forces, it is more difficult to levitate conducting particles (Crane et al., 1981) (Rocke, 1981).
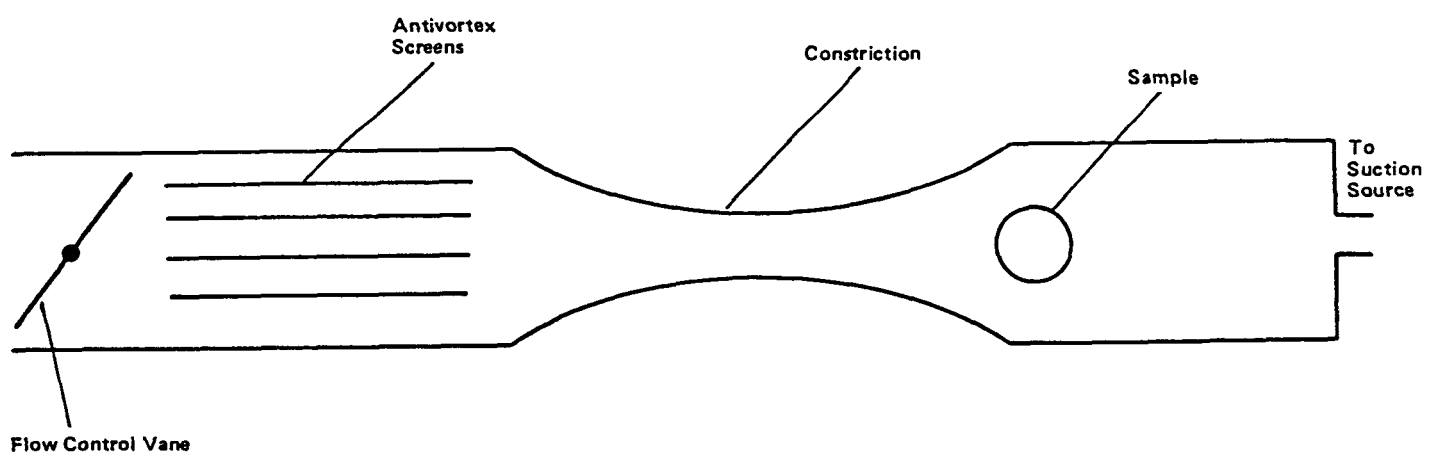
*Figure 3.6.1-1  Constricted-Tube Gas Flow Levitator (Berge, et al., 1981)*
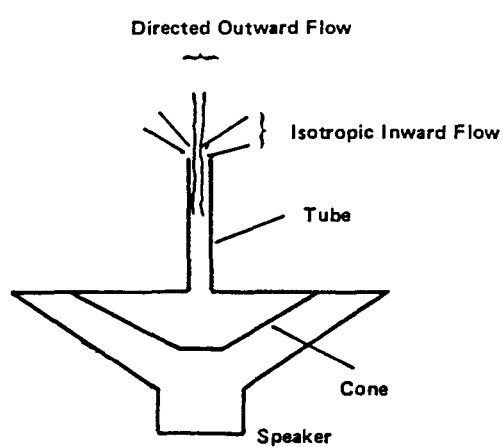
Figure 3.6.2-1  Sonic Pump

## 3.6.4   PLASMA LEVITATION

To study very high temperature (4000 - 10000 K) gas-grain interactions, plasma levitation might be used. One or more plasma torches would be created by passing the gas through induction coils. The particle would be aerodynamically levitated in the tail flame of the plasma torch. An arrangement for 1 g is shown in Fig. 3.6.4-1. (Farnell and Waldie, 1973). In microgravity, constricted tube or triaxial arrangements might be used.

## 3.7   ELECTROMAGNETIC LEVITATION

A conducting particle may be confined at a minimum in an alternating magnetic field. A reversed coil configuration (see Fig. 3.7-1 (a)) (Wang, 1983) produces a cusp shaped field (see Fig. 3.7-1 (b)) (Frost and Change, 1982) which confines the particle at its center. Two limitations with this method are that the particle is heated (and perhaps melted) and that a minimum particle conductivity of 1000 $(ohm-m)^{-1}$ is required (Day and Ray, 1986).
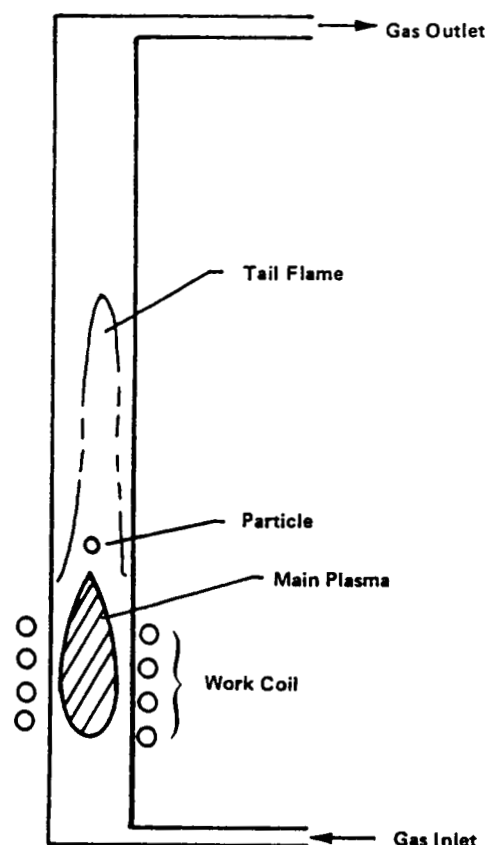
*Figure 3.6.4-1*
*Levitation in 1 g in an Induction Plasma Torch*
*(Farnell and Waldie, 1973)*

Sample ──────➤ ○
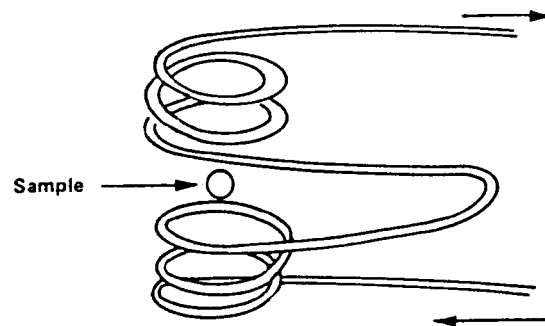
(a) Coil Configuration (Current Direction
for Peak of Half Cycle)

⊗   ⊙
⊗   ⊙ ───── Sample
  ○
⊙   ⊗
⊙   ⊗
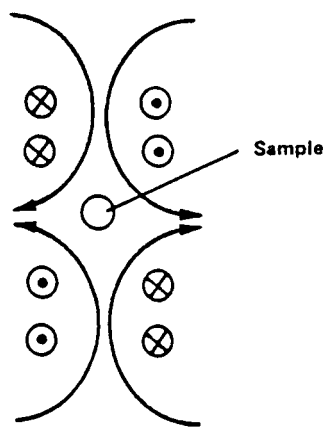
(b) Field Configuration (Current and Field
Direction for Peak of Half Cycle)

*Figure 3.7-1  Simple Configuration for Magnetic Levitation*

## 4.0    LEVITATION INDUCED COAGULATION FORCES

All levitation methods either induce coagulation or otherwise render unrealistic the simulation of multiparticle interactions.

In microgravity levitation forces can be reduced by up to a factor of one million.  However, the effects of Brownian motion would not be reduced at all and for sufficiently small particles the effects of Brownian motion must be as important as those of gravity (see Section 2.3) (aerosols exist in 1 g in the Earth's atmosphere).  Obviously, any levitation scheme that opposes Brownian motion with sufficient strength so as to keep particles away from the walls of the chamber, will fundamentally affect the dynamics of small particles in the confined cloud and will thereby affect the growth of larger particles.

## 4.1    COAGULATION CAUSED BY LIGHT PRESSURE LEVITATION

Multiple liquid drops have been levitated in a vertical beam in 1 g. They become ordered such that the largest is closest to the beam focus.  Also the upper drops are located in the light intensity maxima of the diffraction pattern formed by the lower drops.  Up to 20 drops have become ordered in a fixed array, which rearranges upon being disturbed.  Also, irregularly shaped (solid) objects orient themselves in the beam (Ashkin and Dziedzic, 1975).

While the above phenomena may not be strictly defined as coagulation, they would probably prevent realistic cloud experiments because they would interfere with particle movement and introduce artificial anisotropy and diffraction into light scattering.

Light pressure levitation is the only technique by which "vacusols" might be confined.  But in the absence of Brownian motion, the ordering in fixed arrays would be particularly acute.

## 4.2    COAGULATION CAUSED BY RADIOMETRIC LEVITATION

The TEM01* (doughnut) mode required for radiometric levitation (Lewittes and Arnold, 1982) will cause (or at least enhance) coagulation on the axis of the beam.  Also, highly absorbing carbon particles have been observed to assume stable positions in (highly localized) energy density minima in a focused TEM00 (gaussian) beam (Pluchino, 1983).  In either case radiometric levitation will interfere with realistic cloud experiments.

## 4.3    COAGULATION CAUSED BY ACOUSTIC LEVITATION

Acoustic levitation will cause acoustic agglomeration, the industrial use of which is an intermediate treatment of aerosols that contain submicron- and micron-sized particles so that they may be removed by conventional cleaning techniques.  The high-intensity acoustic field causes local velocity fluctuations, which cause the particles to collide, adhere, and grow (Tiwary, 1984).  This is partly a result of the amplitude of acoustic jitter being dependent on particle size (Foster, 1985) (see Figs. 4.3-1 thru 4.3-3).

It is appropriate to estimate the rate of acoustic agglomeration for a particle that is acoustically levitated in $10^{-5}$ g.  Equating Eq. 2.9-2 to the gravitational force $10^{-5}$ mg, using the maximum value of the term sin 2kx, and solving for the pressure amplitude yields.

$$p_1 = \sqrt{\left(\frac{8}{5}\right)\left(\frac{\rho_g c^2 \rho_p 10^{-5} g}{k}\right)} , \qquad (4.3\text{-}1)$$

where $\rho_g$ is the mass density of the gas and $\rho_p$ is the mass density of the particle.  The sound intensity ("a measure of the acoustic energy flux") is (Foster, 1985)

$$I = \frac{p_1^2}{\rho_g c^2} . \qquad (4.3\text{-}2)$$

The sound intensity level in decibels (dB) is (Foster, 1985)

$$IL = 10 \log_{10}(I/I_o), \qquad (4.3\text{-}3)$$

where $I_o = 10^{-12}$ W/m$^2$.  For air with a pressure of 765 mb and a temperature of 283 K and sound with a frequency of 1000 Hz, Eqs. 4.3-1 thru 4.3-3 yield a sound intensity level of 125 dB.  The rate of acoustic agglomeration will be approximated for water droplets with a mean radius of 12  µm, a radius variance of 1.0, and a total water
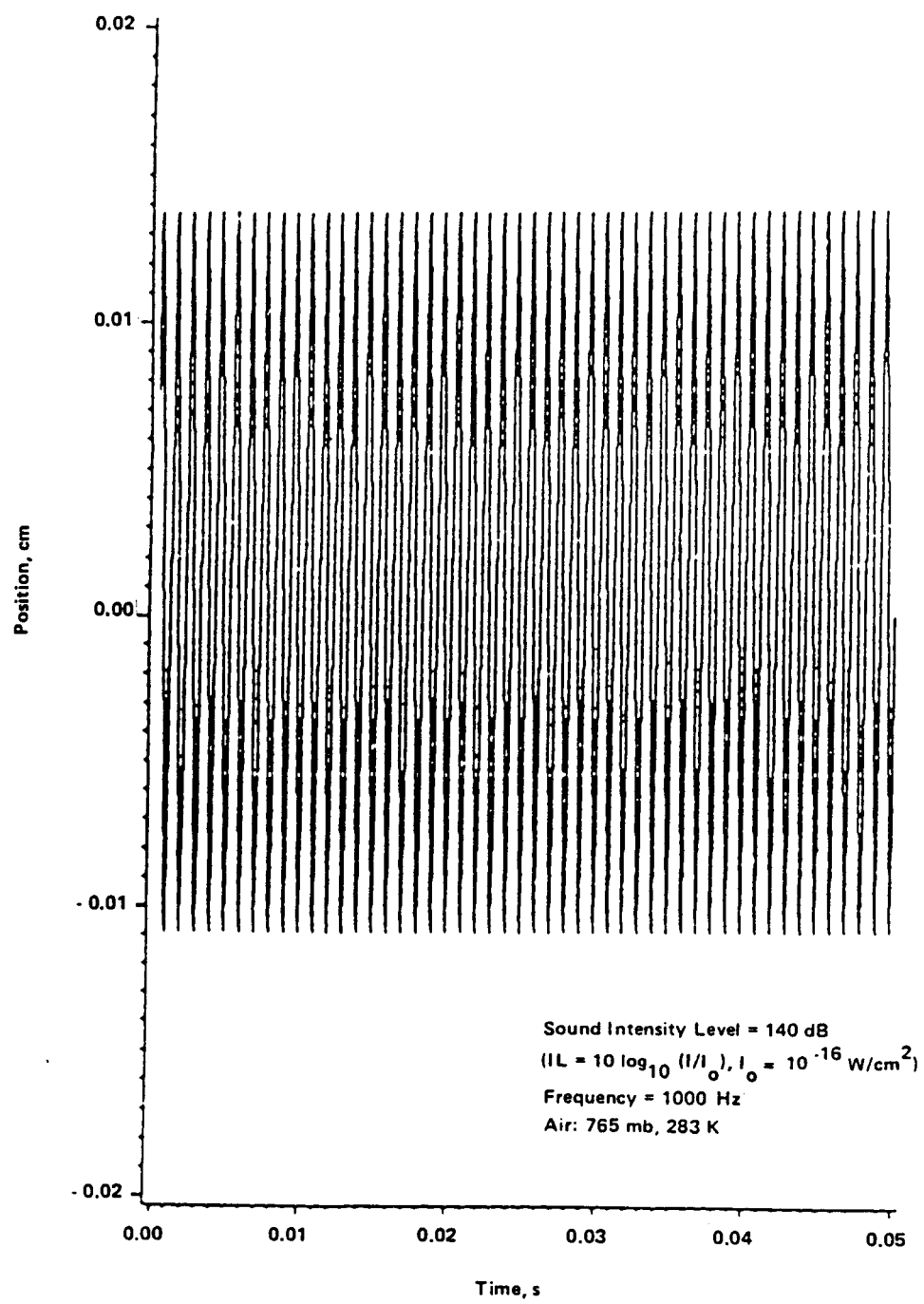
Figure 4.3-1 Motion of a 1-μm Droplet (Foster, 1985)
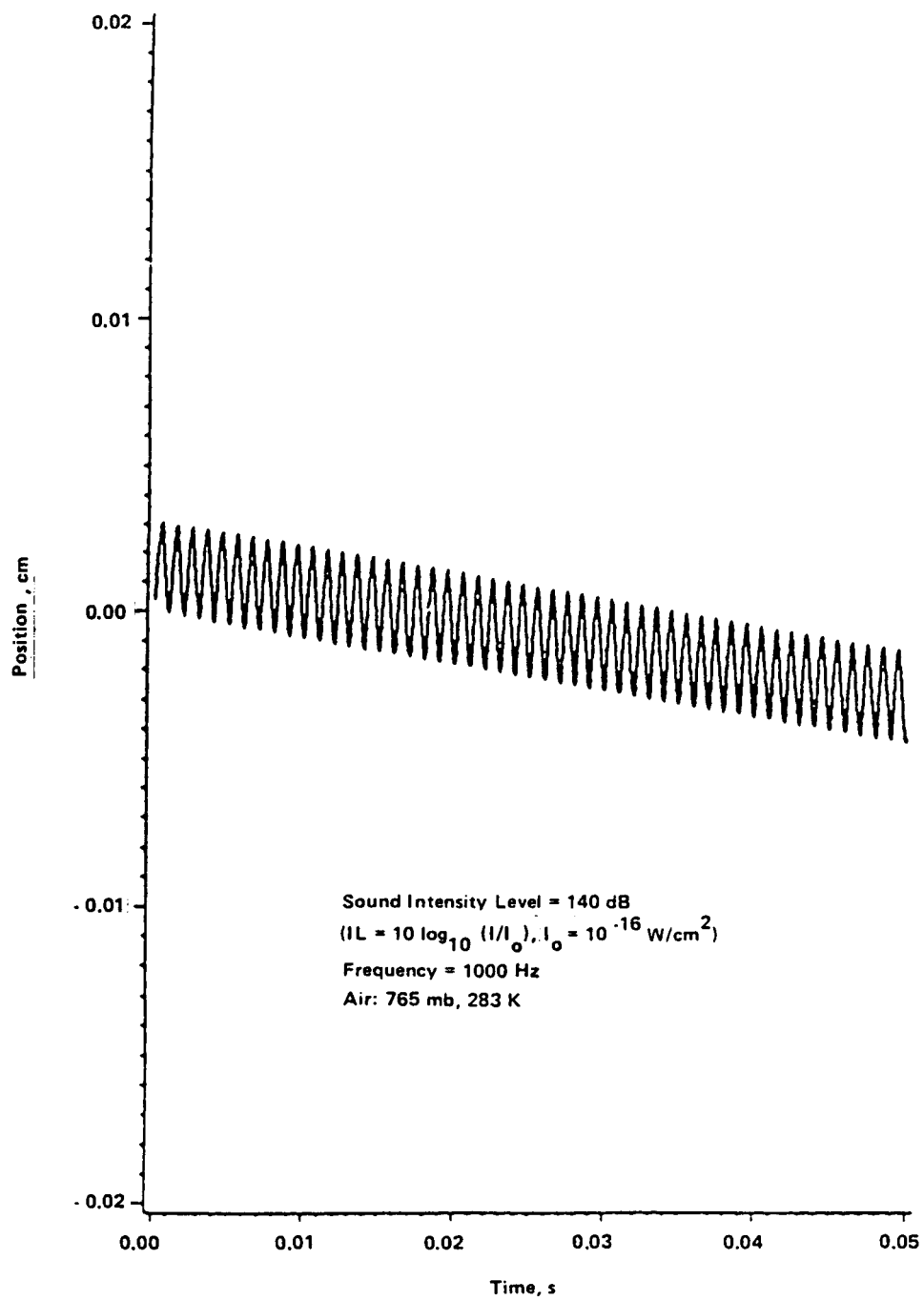
Figure 4.3-2 Motion of a 10 - $\mu m$ Droplet (Foster, 1985)

48
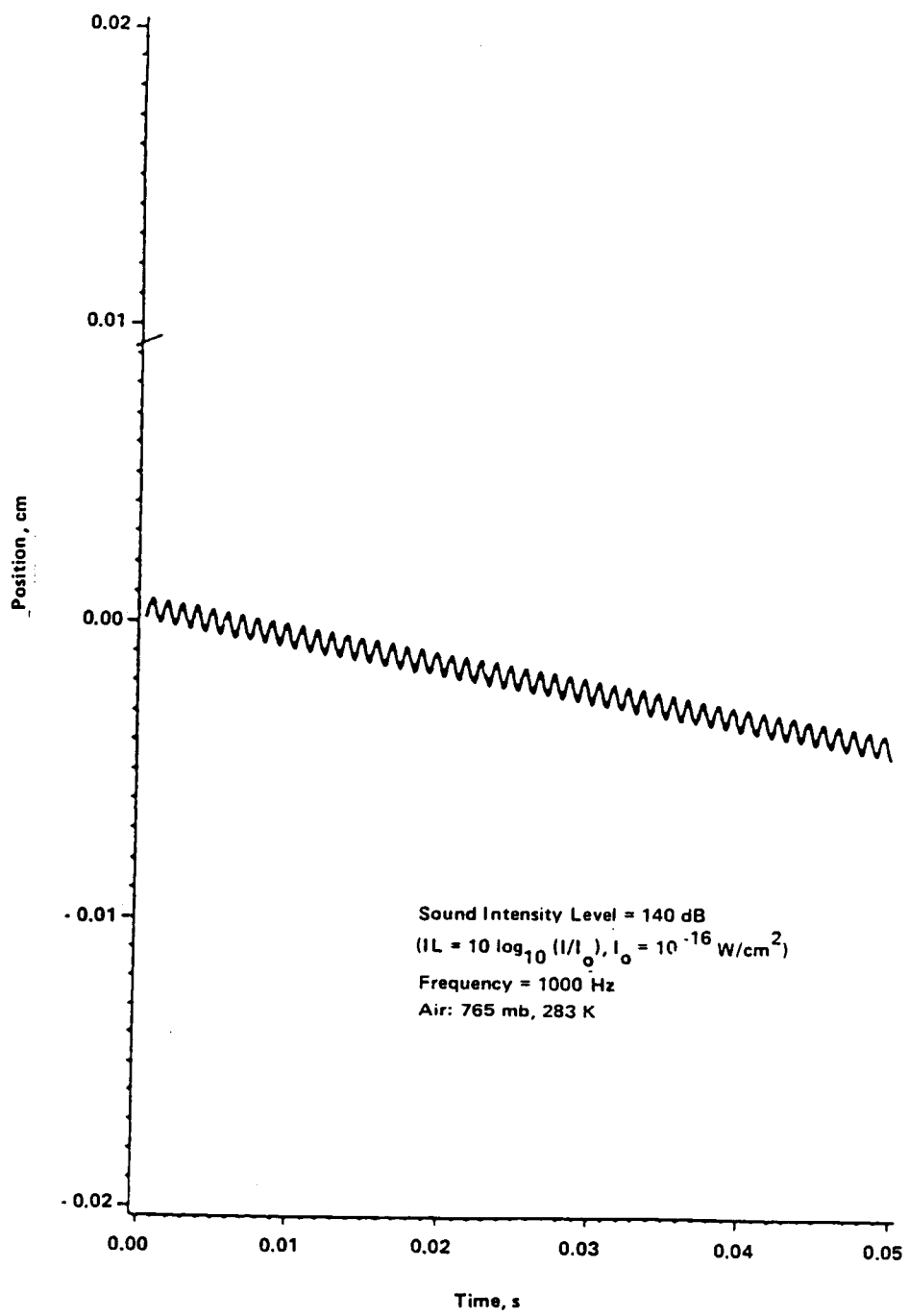
*Figure 4.3-3 Motion of a 20 - μm Droplet (Foster, 1985)*

content of 1 $g/m^3$. Letting n(t) be the total number density with the initial size distribution, the initial variance is sufficiently small that it is approximately true that

$$\frac{dn}{dt} = -n^2 K, \qquad\qquad (4.3\text{-}4)$$

where K is the collection constant for the initial size distribution. [An accurate answer would require the integration of the stochastic collection equation in which K is a collection kernel (Foster, 1985).] For the stated conditions at 125 dB, K = 0.00006 $cm^3$/s (see Fig. 4.3-4) (Foster, 1985). The initial density of droplets is 138/$cm^3$. Therefore, the initial fractional rate of change of the number density of water droplets with the mean initial radius of 12 $\mu m$ is

$$\frac{1}{n}\frac{dn}{dt} = -nK = -0.0083/s = -0.50/\text{minute}.$$

Therefore, in one minute, one-half of the droplets initially present would have agglomerated. The above calculation is extremely crude. One reason for this is that the collection constant used is for traveling waves (Foster, 1985) rather than for the standing waves used in acoustic levitation. However, standing waves are preferred for causing acoustic agglomeration (Barmatz, March 24, 1982).

The kinetic (Brownian) coagulation coefficient (no acoustic agglomeration) for particles with a radius of 12 $\mu m$ is $10 \times 10^{-10}$ $cm^3$/s (Twomey, 1977), which for an initial density of 138/$cm^3$ yields an initial fractional rate of change of -0.36/month. Obviously the acoustic agglomeration overwhelms the kinetic coagulation.

Acoustic agglomeration is not just the same coagulation speeded up. One reason is that acoustic agglomeration is highly dependent upon particle radius (Foster, 1985).

Another point is that for organic chemistry experiments that are scheduled to last days or weeks or months [The Titan aerosol experiment is scheduled to last 90 days (NASA TM-89606, 1987)], acoustic agglomeration would have to be taken into account. Questions of the following kind should be considered: would the over 75 separate compounds comprising the Titan aerosol tholin (Khare, 1984) be formed in the same proportion if agglomerated in a few minutes versus three months?
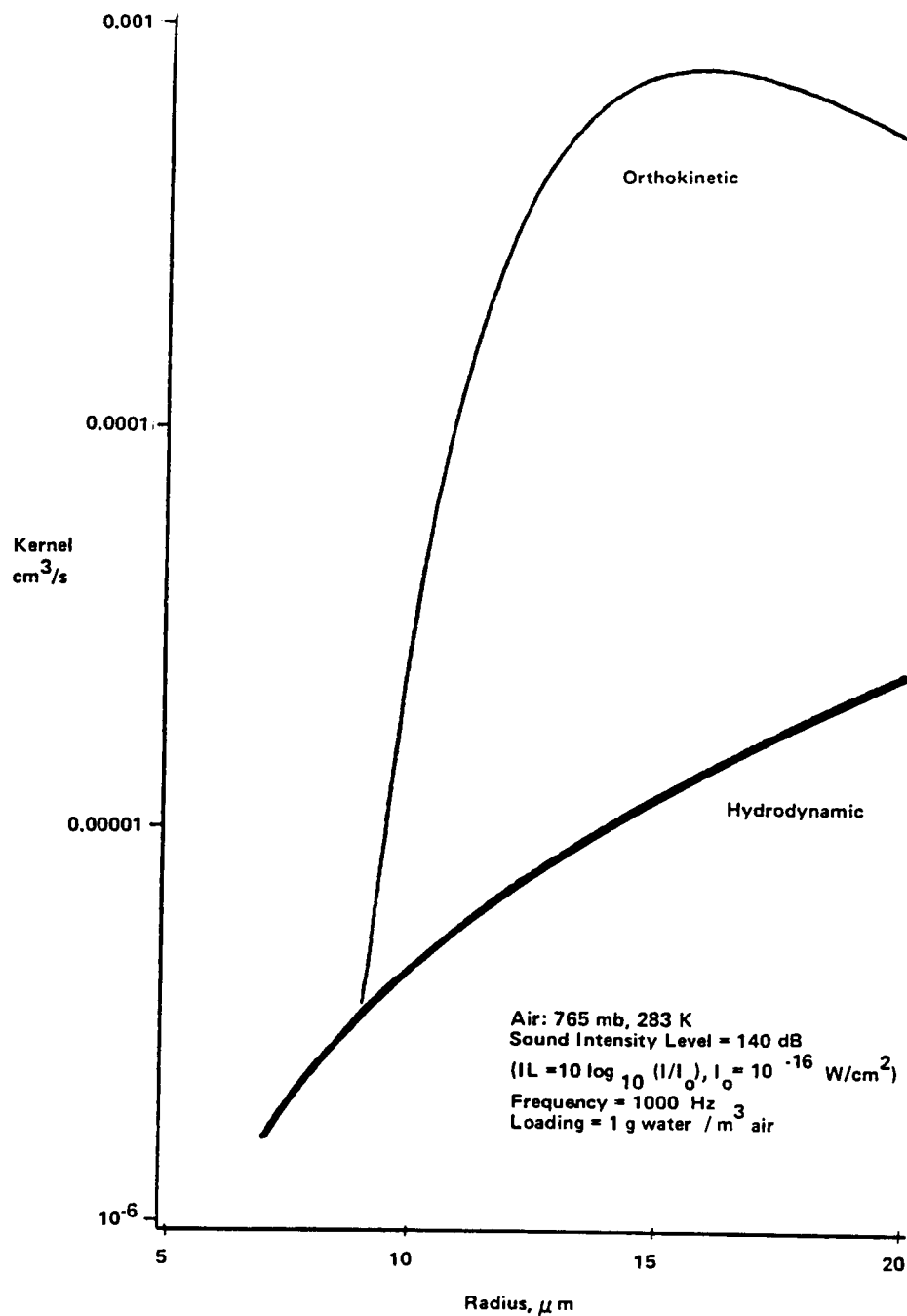
*Figure 4.3-4*
*Acoustic Kernels as a Function of Initial Mean Radius  (Foster, 1985)*

## 4.4    COAGULATION CAUSED BY ELECTROSTATIC LEVITATION

For electrostatic levitation with feedback (eg. tetrahedral electrostatic positioner) only one particle may be levitated and thus coagulation is not defined.

For levitation with alternating electric fields a circular central (alternating voltage) electrode is designed for the levitation of only one particle. A rectangular central electrode can accommodate a number of particles, which are confined to and free to move along the long axis of the rectangle (Straubel and Straubel, 1986). However, since these charged particles are mutually repulsive, even this lack of coagulation in one dimension does not constitute a realistic simulation.

## 4.5    COAGULATION CAUSED BY AERODYNAMIC LEVITATION

Coagulation is not defined for constricted-tube gas-flow levitation or triaxial sonic pump levitation, both of which are designed to levitate single particles.

## 4.6    COAGULATION CAUSED BY ELECTROMAGNETIC LEVITATION

Electromagnetic levitation is designed to levitate a single particle. With more than one particle present, either the system would fail or possibly the particles would coagulate.

## 5.0    FEASIBILITY OF LONG DURATION EXPERIMENTS

Single particle long duration experiments are feasible.  The electrostatic levitation method may require occasional recharging of the particle (eg. by a pulse-charging system).  The only real limiting factor may be the electric power required to maintain the temperature of extremely hot or cold chamber walls.

Since all levitation methods cause coagulation (or introduce some other unrealistic effect) it would probably be best to confine cloud experiments with chemically inactive walls.  The rate of precipitation at the walls would then depend on the surface to volume ratio, which is minimized for large volumes.  Therefore the duration of cloud experiments would be limited by the size of the chamber.  This suggests that two chambers be used:  a small one for single particle experiments and a very large one for cloud experiments.

Fractal formation experiments are feasible because the low density of a large fractal causes its settling due to residual gravity to be very slow.  (See Appendix A for an analysis of fractal coagulation.)

6.0    FEASIBILITY OF CLASSES OF EXPERIMENTS

The feasibility will be analyzed of the following classes of
experiments:

(a) low velocity collision experiments,
(b) experiments to simulate high temperature condensation of refractory
    grains,
(c) cloud coagulation experiments,
(d) experiments to measure optical properties of clouds,
(e) Titan aerosol experiments,
(f) fractal formation experiments,
(g) coating by coagulation experiments, and
(h) "vacusol" experiments.


6.1    LOW VELOCITY COLLISION EXPERIMENTS

The pendelum type collision experiments designed to achieve collision
velocities down to $10^{-2}$ mm/s (based on $10^{-5}$ g residual
acceleration) (Marshall et al., 1985) may not be feasible in general
because of vibrational accelerations of up to $10^{-2}$ g due to astronaut
motion and equipment vibration.  Of course, the motion due to these
vibrational accelerations could be subtracted out, but then the
accuracy of the experiment would be limited by that of the
accelerometers.

A better procedure might be to place the two particles 1 mm apart in
the center of the chamber.  One would be given a small push toward the
other and their collision would be recorded with high speed video
cameras.  Vibrations would affect the camera but would have no effect
on the recorded relative velocity or separation distance of the
particles.  Of course, the residual acceleration would eventually cause
the particles to hit the wall of the chamber, thus ending the
experiment.  For a chamber of radius 5 cm and a residual acceleration
of $10^{-5}$ g, the particles would hit the wall in 32 s.  Thus, for an
initial separation of 1 mm, the minimum closing velocity of the two
particles would be 0.03 mm/s.  This velocity could be decreased by
using a larger chamber.  However, the size of the chamber is probably
limited by the field of view of the cameras, although multiple cameras
might mitigate this problem.

In the above scheme, vibration may still affect the assignment of
initial position and velocity to the particles.  Therefore a given
experiment must be performed many times and only these cases having
initial velocities and positions of interest will be selected for
analyses.

6.2    EXPERIMENTS TO SIMULATE HIGH TEMPERATURE CONDENSATION OF REFRACTORY
       GRAINS

Since all levitation techniques enhance coagulation or cause other
unrealistic effects, condensation experiments should probably not use
levitation but be confined by chemically inactive walls.  During the
experiment a sample would be drawn off and an individual grain would be
electrostatically levitated in a small chamber to study its optical

properties. This sample would also provide grains for physical and chemical analyses and for the measurement of the particle size distribution (see Figure 6.2-1). Once suspended electrostatically the grain could continue to grow. The reason for initial nucleation in a large chamber is to minimize the surface to volume ratio and thereby minimize contamination from the walls.

Pulsed levitation could be used to position a single grain in the large chamber. This could be by laser (radiometric or light pressure) or by gas puffs.

Optical measurements could also be made in the large chamber. Size, number densities, and trajectories of individual particles can be measured and stored or made available in real-time. One technique is the image dissector (Knollenberg, 1979).

## 6.3 CLOUD COAGULATION EXPERIMENTS

These are feasible because they are performed on Earth. The advantage of microgravity is that it affords a lower precipitation rate for large particles.

For condensation/coagulation experiments of the atmospheric type, one should study the cloud chambers designed for the Atmospheric Cloud Physics Laboratory (ACPL), which was designed as a payload for the Space Shuttle. A computerized literature search of the Aerospace Abstracts yields 42 references to ACPL.

For general coagulation experiments the appropriate equations must be solved to determine if the objectives may be obtained within a reasonable time. The time rate of change of total number density is easily obtained by solving the following equation (Ludlam, 1980):

$$\frac{dN}{dt} = -kN^2 , \tag{6.3-1}$$

where

$$k \approx 8\pi r \, D_p \approx 5 \times 10^{-10} \text{ cm}^3/\text{s for air at STP,}$$

r is the particle radius and $D_p$ is the particle diffusion coefficient. The solution is (Ludlam, 1980)

$$N(t) = \frac{1}{1/N_0 + Kt} , \tag{6.3-2}$$

where $N_0$ is the initial number density (see Tables 6.3-1 and 6.3-2). To obtain the evolution of the detailed distribution, the following equation must be solved numerically (Twoney, 1977):

$$\frac{d}{dt} n(x) = -n(x) \int_0^\infty K(x,v) \, n(v) \, dv$$

$$+ \frac{1}{2} \int_0^x K(x-v,v) \, n(x-v) \, n(v) \, dv, \tag{6.3-3}$$
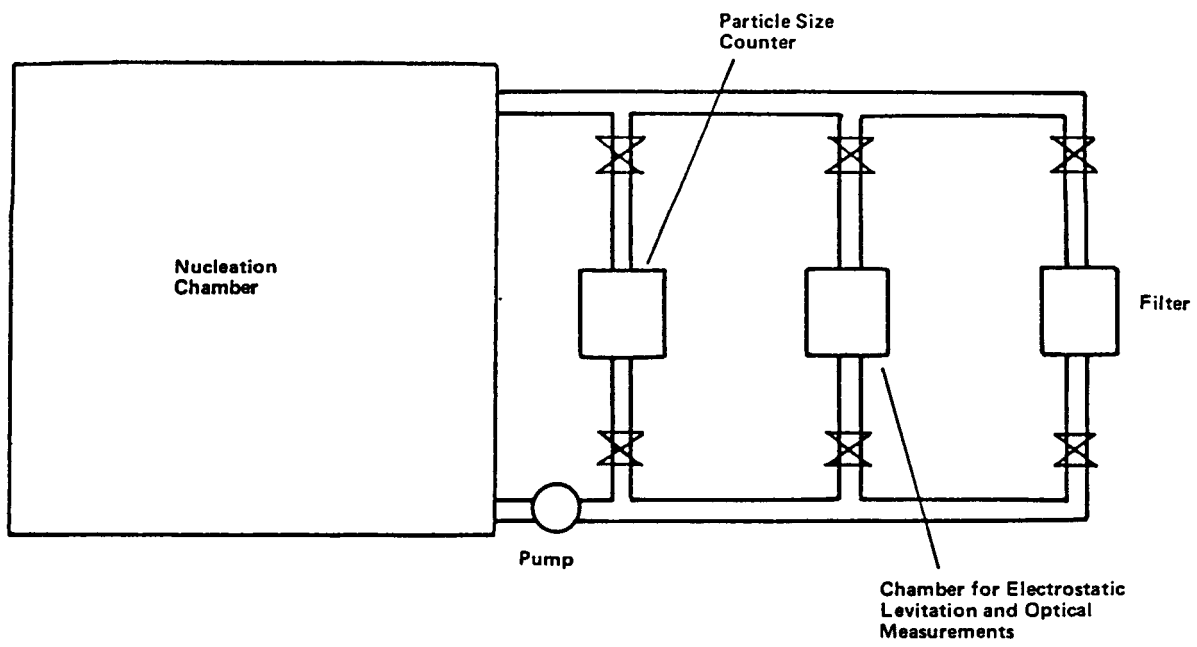
Figure 6.2-1 Layout for High-Temperature Condensation of Refractory Grains

where

$n(x)$   =   number density per unit particle volume for particles of volume $x$ ($m^{-6}$), and

$K(x,v)$   =   coagulation kernel ($m^3 s^{-1}$).

For coagulation resulting from Brownian motion, $K$ may be written (as a function of particle radius) as follows (Twomey, 1977):

$$K(r_1, r_2) = 4 \pi (r_1 + r_2) (D_1 + D_2). \qquad (6.3\text{-}4)$$

As the Knudsen number approaches zero (Twomey, 1977),

$$D = \frac{kT}{6 \pi \mu_g r}, \text{ and} \qquad (6.3\text{-}5)$$

$$K(r_1, r_2) = \frac{2kT}{3 \mu_g} (r_1 + r_2) \left( \frac{1}{r_1} + \frac{1}{r_2} \right). \qquad (6.3\text{-}6)$$

Table 6.3-1

Time t Required to Reduce an Initial Concentration $n_0$ ($cm^{-3}$) of
Small Particles of Uniform Size to $n_0/10$ under Ordinary Conditions at
STP (LUDLAM, 1980)

| $n_0$ ($cm^{-3}$) | t |
|---|---|
| $10^{11}$ | 0.2 sec |
| $10^6$ | 5 hr |
| $10^5$ | 2 days |
| $10^4$ | 3 wk |
| $10^3$ | 6 mo |

TABLE 6.3-2

Change of Concentration of Small Particles of Uniform Size During
One Week, Under Ordinary STP Conditions (LUDLAM, 1980).

| $n_0$ ($cm^{-3}$) | n ($cm^{-3}$) |
|---|---|
| $10^{12}$ | $2.9 \times 10^3$ |
| $10^8$ | $2.9 \times 10^3$ |
| $10^4$ | $2.2 \times 10^3$ |
| $2.2 \times 10^3$ | $1.3 \times 10^3$ |

Whenever possible, cloud coagulation experiments probably should not use levitation but should use confinement by inert walls. In order to minimize the effect of wall losses, the chamber volume and the initial density should be as large as possible. On Earth smog chambers of volume 60 $m^3$ fabricated of FEP Teflon film are used to study aerosol formation and even in these large chambers a significant fraction of the particles is lost to the walls (McMurry and Grosjean, 1985).

In addition to particle loss to the walls by Brownian diffusion and residual acceleration, turbulent diffusion and electrostatic drift must be considered (McMurry and Rader, 1985). The effect of turbulent diffusion in microgravity has not been investigated during the present study. Electrostatic drift could probably be eliminated by grounding a dielectric chamber at numerous points.

Another consideration is loss to the walls of the gas-phase species (according to McMurry and Grosjean, 1985):

> Wall deposition of gas-phase species may also affect experimental results. The chemical systems that are studied in smog chambers are typically complex, involving many gas-phase species. The time dependence of any given species depends on its rates of formation and consumption by other species. Wall-deposition rates probably vary from species-to-species and thus introduce another removal rate in the differential equations that must be solved to determine the time history of the species. If wall-deposition rates are comparable or large compared to rates at which a species is consumed by chemical reactions, then wall deposition may affect the time history of this and other species.

Since loss rate to the walls of gaseous or particulate species is proportional to number density, while rate of particulate coagulation is proportional to the square of number density, obviously there can be no generalized comparison between these two mechanisms of particle removal.

## 6.4    EXPERIMENTS TO MEASURE OPTICAL PROPERTIES OF CLOUDS

Optical properties of individual particles have conveniently been measured on Earth via light pressure levitation for transparent particles (Lettieri and Preston, 1985) (Ashkin and Dziedzic, 1981) and via electrostatic levitation for transparent and nontransparent particles (Weiss-Wrana, 1983) (Straubel and Straubel, 1986). These experiments could easily be performed in microgravity with an advantage being that a liquid droplet would be more nearly spherical when not levitated against 1 g. Also, in microgravity the laser levitation would cause less heating and evaporation and electrostatic levitation would require less charge.

The optical measurement techniques listed below were obtained from a review paper by Hirleman (Hirleman, 1983). The techniques described are all non-intrusive, offering minimal disturbance to the system being studied.

Photography and holography are useful for particles greater than about five microns in diameter. They may be automated to determine a mean particle diameter, the particle size distribution and concentration, as well as specific information such as particle shape (Simmons, 1977) (Fleeter et al., 1982) (Knollenberg, 1977). Using double flash photography, in which two closely spaced light pulses are used, the particle velocity may be obtained as well (Lennert et al., 1977). Pulsed holographic techniques produce three-dimension information on particle size and shape (Trolinger, 1980) (Thompson, 1974) (Jones, 1977).

A single particle counter is an instrument which shines a laser into a relatively small optical sample volume traversed by the particles to be measured, and collects scattered light at one or more scattering angles. The particle size distribution may be inferred from the intensity and/or angular distributions of the scattered light. This technique is capable of measuring particle sizes of 0.5 microns and above with high specificity (Ungut et al., 1978) (Knollenberg, 1977) (Holve and Self, 1979). With a second laser beam, one also has the potential for simultaneous velocity measurements (Hirleman, 1978).

Particle sizing interferometry is a method of particle sizing which incorporates laser Doppler velocimetry. In the latter technique, a laser beam is split, with the two component beams intersecting a sample volume at different angles. A particle passing through the sample volume will scatter each beam with a distinct Doppler shift. The difference of the scattered frequencies, which contains particle velocity information, is obtained by heterodyning the scattered signals. In particle sizing interferometry, the size of the particle is then determined, (in an average way, since the particle doesn't always traverse the center of the sample volume) from the product of the particle velocity, with the time over which the scattered signal was received (Farmer, 1972) (Fristium et al., 1973) (Robinson and Chu, 1975) (Chu and Robinson, 1977) (Yule et al., 1977) (Farmer, 1978) (Bachalo, 1980).

An instrument for ensemble or multiparticle analysis is the polar nephelometer (Hansen and Evans, 1980) (Hansen, 1980), which is capable of measuring molecular as well as particulate scattering. In this method, light scattering is measured at several angles, and the scattering intensities are compared to theoretical values based upon Mie theory. In principle, a mean scattering diameter, the particle size distribution, and the real and imaginary parts of the index of refraction may be evaluated in this manner. A similar technique for larger particles, in which the particle size distribution is determined from measurements on the forward scattering lobe, is laser diffraction particle sizing (Hirleman, 1983) (Chin et al., 1985) (Swithenbank et al., 1977) (Dobbins et al., 1963) (Roberts and Webb, 1964) (Dieck and Roberts, 1970) (Alger, 1979).

In diffusion broadening spectroscopy, particle sizes for very small particles are determined from their diffusion constants, as measured from Doppler shifts due to Brownian motion (Benedek, 1969) (Penner et al., 1976) (King et al., 1982). This technique has the advantage of not requiring knowledge of the index of refraction.

Finally, when the index of refraction and the volume concentration of the particles are known, the volume-to-surface-area mean diameter (or Sauter Mean Diameter, $D_{23}$) of the particle distribution may be determined by a single transmittance measurement (Dobbins, 1966).

## 6.5    TITAN AEROSOL EXPERIMENTS

As currently proposed the Titan aerosol experiment (McKay, 1986) is not feasible. $N_2$ at the specified pressure of 0.2 mb has a mean free path of $3 \times 10^{-4}$ m, which is the minimum particle size for acoustic levitation (McKay, 1986). For laser light with a wavelength of 6888 angstroms, a tholin particle of this size is almost opaque (khare, 1984). For optical levitation against an acceleration of $10^{-5}$ g, the absorbing power would be $4 \times 10^{-4}$ W. Assuming an emissivity for thermal radiation of 0.1 results in a steady state temperature of 700 K, which is probably above the starting decomposition temperature for tholin. One solution might be to raise the gas pressure, which would lower the mean free path and thereby decrease the minimum size for acoustic levitation. An obvious problem with this solution is that raising the pressure may change the kinetics or even the fundamental chemistry of tholin formation.

Another problem is that when the mean free path of the gas is equal to the particle size, the radiometric (photophoretic) force is maximized (Ashkin and Dziedzic, 1976). For an absorbing particle such as tholin, the radiometric force may exceed the force from light pressure. For an incident power P, the photon pressure force is (Lewittes and Arnold, 1982).

$$F_p = \frac{P}{c} .$$
(6.5-1)

Neglecting the thermal conductivity of the particle and the cooling of the particle by radiation, an opaque particle that is much smaller than the mean free path experiences a radiometric force of (Lewittes and Arnold, 1982).

$$F_r = \frac{P}{3v} ,$$
(6.5-2)

where v is the molecular velocity. The ratio of forces is

$$\frac{F_r}{F_p} = \frac{c}{3v} .$$
(6.5-3)

At 300 K the velocity of $N_2$ molecules is 300 m/s and therefore the radiometric force exceeds the force due to photon pressure by a factor of $3 \times 10^5$.

A crude calculation shows that the radiometric force can be this large even at the low pressure of 0.2 mb. At 0.2 mb and 300 K the number density is $4.83 \times 10^{21}$ m$^{-3}$ and the cross section of a $3 \times 10^{-4}$ m diameter particle will encounter $1.02 \times 10^{17}$ collisions per second with the gas. Assuming a particle mass density of water, the levitation force at $10^{-5}$ g must be $1.38 \times 10^{-12}$ Nt, which for light pressure levitation would require a power of $4 \times 10^{-4}$ W. To remove this heat the $N_2$ molecules would have to leave the lighted surface of the particle at a speed of 509 m/s yielding a radiometric force of $10^{-6}$ Nt. Thus, in this very crude calculation, which is based on the specified pressure, the radiometric force exceeds the force due to photon pressure by a factor of one million.

The problem with confinement via the radiometric force is that the particles would move toward a light minimum, requiring the use of the TEM01* (doughnut) mode. Also, very small particles would be subject to negative photophoresis and would move toward the laser, while large particles would be subject to positive photophoresis and would move away from the laser. Thus as the particle grew the direction of force would change.

A possible way to do this experiment is to let very small tholin particles form in a large chamber with no levitation. These would be suspended by Brownian motion. A gas sampling tube would then transfer a single particle to a small electrostatic levitation chamber (as in Figure 6.2-1), where the particle would continue to grow. A possible problem is that the artificial charge on the levitated particle may interfere with the chemistry of tholin production.

Another possible method is to use occasional pulses of laser light to position a single particle as it continues to grow.

## 6.6  FRACTAL FORMATION EXPERIMENTS

These experiments are feasible and are mentioned in Section 5.0 and analyzed in Appendix A.

## 6.7  COATING BY COAGULATION EXPERIMENTS

An experiment has been proposed in which a particle of initial radius 0.2 μm grows to 0.4 μm by coagulation with 0.1 μm particles and in doing so entrains an organic condensate and shields this organic material from electromagnetic radiation. This experiment would be performed in air at STP and is proposed to last 1-100 hours with a constant density of $1-10^5$/cm$^3$ of 0.1 μm particles.

The chemical feasibility of the entrainment of the organic material is beyond the scope of the present study. The physical feasibility of the coating by coagulation depends on the number density of 0.1 μm particles. The volumetric rate of growth of the big particle is (from Twomey, 1977):

$$\frac{dV_1}{dt} = 4\pi(D_1 + D_2)(r_1 + r_2)\, n_2 \frac{4}{3}\pi r_2^3 , \qquad (6.7\text{-}1)$$

where

$$D_1 = \frac{kT}{6\pi\eta\, r_1} , \qquad (6.7\text{-}2)$$

$$D_2 = \frac{kT}{6\pi\eta\, r_2} , \qquad (6.7\text{-}3)$$

$\eta$ = gas viscosity, and

$n_2$ = number density of small particles.

Since $r_1 > r_2$, $D_2 > D_1$ and (6.7-1) becomes

$$\frac{d}{dt}\left(\frac{4}{3}\pi r_1^3\right) \approx \frac{2\,kT}{3\,\eta\, r_2}\, r_1\, n_2 \frac{4}{3}\pi r_2^3 ,$$

$$r_1 \frac{dr_1}{dt} \approx \frac{2\,kT}{9\,\eta}\, n_2\, r_2^2 . \qquad (6.7\text{-}4)$$

Integrating (6.7-4) from initial radius $r_{1i}$ to final radius $r_{1f}$ yields

$$t \approx \frac{9\eta\,(r_{1f}^2 - r_{1i}^2)}{4\,kT\, n_2\, r_2^2} , \qquad (6.7\text{-}5)$$

$$t \approx 1.16\times10^{17}/n_2 \ [\text{m}^{-3}] . \qquad (6.7\text{-}6)$$

Using the maximum number density of $10^5/\text{cm}^3$ yields t = 1.16 x $10^6$ s = 13 days. Therefore the experiment is not feasible for the given density, duration, and particle sizes.

6.8    "VACUSOL" EXPERIMENTS

"Vacusol" experiments that last more than 30 seconds are not feasible because with no gas present, even the smallest particles will be accelerated at $10^{-5}$ g toward the walls.

## 9.0    SUMMARY AND RECOMMENDATIONS

The results of this study may be summarized as follows:

(a) All levitation techniques either produce artificial coagulation, ordering, or other effects that adversely affect cloud experiments. Therefore, whenever possible, cloud experiments should not use levitation but should be performed in a chamber with inactive walls (eg. Teflon). The chamber should be as large as possible in order to reduce the surface to volume ratio and thereby reduce contamination from the walls.

(b) Levitation is useful for the study of the optical properties of a single particle after it has been nucleated in the large chamber. It may be possible to levitate this single particle during continued growth. Levitation would be performed in a small separate chamber. Electrostatic levitation is a well established technique that is probably the most versatile with respect to particle size and composition.

(c) Pendelum-type low velocity collision experiments are not feasible because the vibrational accelerations of $10^{-3} - 10^{-2}$ g would overwhelm the residual gravity of $10^{-5}$ g. However, sufficiently low collision velocities could be achieved without a pendelum by positioning two particles at the center of the chamber and 1 mm apart, giving one a small velocity toward the other, and recording their relative motion with a high speed video camera.

(d) Refractory grain experiments are feasible if small grain sizes are acceptable.

(e) Cloud coagulation experiments are feasible, in general. However, the feasibility of any particular experiment depends on having sufficiently high initial number density.

(f) Measurement of optical properties of clouds is feasible.

(g) As originally proposed, the Tital aerosol experiment is not feasible if large particle sizes are required. Proposed modifications may enhance its feasibility.

(h) Fractal growth experiments are feasible.

(i) The experiment for particle coating by coagulation is not feasible for the specified number density, duration, and particle sizes.

(j) "Vacusol" experiments lasting more than 30 seconds are not feasible.

The primary recommendation is that as part of, or prior to any engineering feasibility study, the scientific feasibility of each proposed experiment should be analyzed in more detail by the appropriate specialists. Depending on the experiment, this analysis may require accurate numerical simulations (eg. solving the integro-differential coagulation equation) or laboratory work on Earth.

BIBLIOGRAPHY

Alger, T. W., "Polydisperse-particle Size Distribution Function
    Determined from Intensity Profile of Angularly Scattered Light,"
    Applied Optics, V. 18, p. 3494, (1979).

Ashkin, A., "The Pressure of Laser Light," Scientific American, Vol.
    226, Feb. 1972, p. 63.

Ashkin, A. and Dziedzic, J. M., "Observation of Optical Resonances of
    Dielectric Spheres by Light Scattering," Applied Optics, Vol. 20,
    No. 10, 15 May 1981, p. 1803.

Ashkin, A. and Dziedzic, J. M., "Optical Levitation in High Vacuum,"
    Applied Physics Letters, Vol. 28, No. 6, 15 March 1976, p. 333.

Ashkin, A. and Dziedzic, J. M., "Optical Levitation of Liquid Drops by
    Radiation Pressure," Science, Vol. 187, 21 March 1975, p. 1073.

Ashkin, A. and Dziedzic, J. M., "Observation of Light Scattering from
    Nonspherical Particles using Optical Levitation," Applied Optics,
    Vol. 19, No. 5, 01 March 1980, p. 660.

Ashkin, A. and Dziedzic, J. M., "Observation of Radiation-Pressure
    Trapping of Particles by Alternating Light Beams," Physical Review
    Letters, Vol. 54, No. 12, 25 March 1985, p. 1245.

Ashkin, A. et al., "Observation of a Single-Beam Gradient Force Optical
    Trap for Dielectric Particles," Optics Letters, Vol. 11, No. 5,
    May 1986, p. 288.

Bachalo, W. D., "Method for Measuring the Size and Velocity of Spheres
    by Dual-Beam Light-Scatter Interferometry," Applied Optics, V. 19,
    pp. 363-370 (1980).

Barengoltz, J. and Edgars, D., The Relocation of Particle Contamination
    During Spaceflight, TM 33-737 (Pasadena, CA:  Jet Propulsion
    Laboratory, Sept. 1975).

Barmatz, M. B., "Acoustic Levitation with one Transducer," NASA Tech
    Briefs, Vol. 11, No. 6, June 1987, p. 68.

Barmatz, M., "Overview of Containerless Processing Technologies," in
    Materials Processing in the Reduced Gravity Environment of Space,
    edited by G. E. Rindome (New York:  Elsevier Science Publishing
    Co., Inc., 1982), p. 25.

Barmatz, M. et al., "Experimental Investigation of the Scattering
    Effects of a Sphere in a Cylindrical Resonant Chamber," J. Acoust.
    Soc. Am., Vol. 73, No. 3, March 1983, p. 725.

Barmatz, M. B., Acoustic Agglomeration Methods and Apparatus,
    Patent Application (NASA), NASA-Case-NPO-15466-1 (Pasadena, CA:
    Jet Propulsion Laboratory, March 24, 1982).

Benedek, G. B., Polarization, Matter, and Radiation, Presses
    Universitaires de France, Paris, 1969.

Berge, L. H. et al., "Levitator for Containerless Processing," NASA
    Tech Briefs, Spring 1981, p. 105.

Burtscher, H. and Schmidt-Ott, A., "Enormous Enhancement of van der
    Waals Forces between Small Silver Particles," Physical Review
    Letters, Vol. 48, No. 25, 21 June 1982, p. 1734.

Burtscher, H. and Schmidt-Ott, A., "Experiments on Small Particles in
    Gas Suspensions," Surface Science, Vol. 156, 1985, p. 735.

Chin, J. H., Sliepcevich, C. M., and Tribus, M., "Determination of
    Particle Size Distributions in Polydisperse Systems by Means of
    Measurements of Angular Variation of Intensity of Forward Scattered
    Light at Very Small Angles", J. Phys. Chem. Ithaca, V. 5, p. 841,
    (1955).

Chu, W. P. and Robinson, D. M., "Scattering from a Moving Spherical
    Particle by Two Crossed Coherent Plane Waves," Applied Optics, V.
    16, p. 619, (1977).

Corn, M., "Adhesion of Particles," Aerosol Science, ed. by C. N. Davies
    (New York: Academic Press, 1966), p. 359.

Crane, J. K. et al., The Use of Molecular Beams to Support Microspheres
    During Plasma Coating, UCRL-84488 (Livermore, CA: Lawrence
    Livermore National Laboratory, 1981).

CRC Press, Handbook of Chemistry and Physics, 63 ed., edited by
    R.C. Weast and M.J. Astle (Boca Raton, Florida: CRC Press, Inc.,
    1982).

Czarnecki, J. and Itschenskij V., "Van der Waals Attraction Energy
    between Unequal Rough Spherical Particles," Journal of Colloid and
    Interface Science, Vol. 98, No. 2, April 1984, p. 590.

Day, D. E. and Ray, C. S., "Research on Containerless Melts in Space,"
    in Opportunities for Academic Research in a Low-Gravity
    Environment, ed. by G. A. Hazelrigg and J. M. Reynolds (New York:
    American Institute of Aeronautics and Astronautics, Inc., 1986), p.
    165.

Derjaguin, B. V. and Smilga, V., J. Appl. Phys., Vol. 38, p. 4609.

Dieck, R. H. and Roberts R. L., "The Determination of the Sautor Mean
    Droplet Diameter in Fuel Spray Nozzles," Applied Optics, V. 9, pp.
    2007-2014, (1970).

Dobbins, R. A. and Jizmagian, G. S., J. Opt. Soc. Am., V. 56, p. 1351
    (1966).

Dobbins, R. A., Crocco, L. and Glassmann, I., "Measurement of Mean
    Particle Sizes of Sprays for Diffractively Scattered Light" AIAA
    Journal, V. 1, pp. 1882-1906, (1963).

Dunn, S. A., Development of the Sonic Pump Levitator, Final Report, NASA CR-171382 (Madison, Wis: Bjorksten Research Laboratories, Inc., February 28, 1985).

Farmer, W. M., "Measurement of Particle Size, Number Density, and Velocity Using a Laser Interferometer," Applied Optics, V. 11, p. 2603, (1972).

Farmer, W. M., "Measurement of Particle Size and Concentrations Using LDV Techniques", in Proceedings of the Dynamic Flow Conference, 1978.

Farnell, G. A., and Waldie, B., "A Levitation Technique for Exposing a Single Particle or Group of Particles to High Temperature Gases," Journal of Physics E. Scientific Instruments, Vol. 6, No. 2, Feb. 1973, p. 137.

Fleeter, R., Toaz, R., and Sarohia, V., "Application of Digital Image Analysis Techniques to Antimisting Fuel Spray Characterization," ASME Paper 82-WA/HT-23, American Society of Mechanical Engineers, New York, 1982.

Foster, M. P., The Behavior of Cloud Droplets in an Acoustic Field: A Numerical Investigation, AD 1-A163 704, Report Number ASL-TR 1-0181 (White Sands Missile Range, NM: U.S. Army Atmospheric Sciences Laboratory, August 1985).

Fristium, R. M., Jones, A. R., Schwar, M. S. R., and Weinberg, F. S., "Particle Sizing by Interference Fringes and Signal Coherence in Doppler Velocimetry," Faraday Symposia of the Chemical Society, V. 1, p. 183, (1973).

Frost, R. T. and Change, C. W., "Theory and Applications of Electromagnetic Levitation," in Materials Processing in the Reduced Gravity Environment of Space, ed. by G. E. Rindome (New York: Elsevier Science Publishing Company, Inc., 1982), p. 71.

Gammell, P. M. et al., Stabilized Acoustic Levitation of Dense Materials Using a High-Powered Siren, JPL Publication 82-92 (Pasadena, CA: Jet Propulsion Laboratory, December 15, 1982).

Gregory, J., "Approximate Expressions for Retarded van der Waals Interaction," Journal of Colloid and Interface Science, Vol. 83, No. 1, Sept 1981, p. 138.

Halliday, D. and Resnick, R., Physics, Part II (New York: John Wiley & Sons, Inc., 1962)

Hansen, M. A., and Evans, W. H., "Polar Nephlometer for Atmospheric Particulate Studies", Applied Optics, V. 19, pp. 3389-3395 (1980).

Hansen, M. Z., "Atmospheric Particulate Analysis using Angular Light Scattering", Applied Optics, V. 19, pp. 3441-3448 (1980).

Hatano, H. et al., "Ultrasonic Levitation and Positioning of Samples," Proceedings of 2nd Symposium on Ultrasonic Electronics, Tokyo 1981, Japanese Journal of Applied Physics, Vol. 21 (1982) Supplement 21-3, p. 202.

Hidy, G. M., Aerosols, an Industrial and Environmental Science (Orlando, Florida: Academic Press, 1984).

Hirleman, E. D., "Laser Technique for Simultaneous Particle Size and Velocity Measurements," Optics Letters, V. 3, pp. 19-21, (1978).

Hirleman, E. D., "Noninstrusive Laser-Based Diagnostics", AIAA-83-0549 conference paper, AIAA Jan 10-13, 1983, Reno, Nevada.

Hirleman, E. D., "On-line Calibration Technique for Laser Diffraction Droplet Sizing Instruments", ASME Paper 83-GT-232, 20th International Gas Turbine Conference, March 27-31, 1983, Pheonix, AZ.

Holve, D. and Self, S. A., "Optical Particle Sizing for in situ Measurements, Parts I and II," Applied Optics, V. 18, pp. 1632-1652, (1979).

Hough, D. B. and White, L. R., "The Calculation of the Hamaker Constants from Lifshitz Theory with Application to Wetting Phenomena." Advances in Colloid and Interface Science," Vol. 14, 1980, p. 3.

Jones, A. R., J. Physics D., V. 10, pp. L163-L165 (1977).

Khare, B. N. et al., "Optical Constants of Organic Tholins Produced in a Simulated Titanian Atmosphere: From Soft X-Ray to Microwave Frequencies," Icarus, Vol. 60, 1984, p. 127.

King, G. B., Sorenson, C. M., Lester, T. W., and Merklin, J. F., "Photon Correlation Spectroscopy used as a Particle Size Diagnostic in Sooting Flames", Applied Optics, V. 21, pp. 976-978 (1982).

Knollenberg, R. G., "Image Dissector for Size and Position of Statically Suspended Particles," Applied Optics, Vol. 18, No. 21, 1 Nov 1979, p. 3602

Knollenberg, R. G., "The Use of Low Power Lasers in Particle Size Spectroscopy," in Practical Applications of Low Power Lasers, pp. 137-152, SPIE V. 92, 1977.

Lennert, A. E., Sowls, R. E., Belz, R. A., Goethert, W. H., and Bentley, H. T., "Electro-optical Techniques for Diesel Engine Research", Experimental Diagnostics in Gas Phase Combustion, (B. T. Zinn, ed.) pp. 629-656. American Institute of Aeronautics and Astronautics, 1977.

Lee, M. C., and Feng, I., "Acoustic Levitating Apparatus for Submillimeter Samples," Rev. Sci. Instrum., Vol. 53, No. 6, June 1982, p. 854.

Lettieri, T. R. and Preston, R. E., "Observation of Sharp Resonances in the Spontaneous Raman Spectrum of a Single Optically Levitated Microdroplet," Optics Communications, Vol. 54, No. 6, 15 July 1985, p. 349.

Lewittes, M. and Arnold, S., "Radiometric Levitation of Micron Sized Spheres, " Applied Physics Letters, Vol. 40, No. 6, 15 March 1982, p. 455.

Ludlam, F. H., Clouds and Storms (University Park, PA: The Penn. State Univ. Press, 1980).

Makin, B. et al., "Performance Characteristics of a Pulse-Charging System," IEEE Transaction on Industry Applications, Vol. IA-22, No. 3, May/June 1986, p. 542.

Marlow, W. H., "Lifshitz-van der Waals Forces in Aerosol Particle Collisions. I. Introduction: Water Droplets," J. Chem. Phys., Vol. 73, No. 12, 15 Dec. 1980, p. 6288.

Marlow, W. H., "Derivation of Aerosol Collision Rates for Singular Attractive Contact Potentials," J. Chem. Phys., Vol. 73, No. 12, 15 Dec. 1980, p. 6284.

Marlow, W. H., "Survey of Aerosol Interaction Forces," in Aerosol Microphysics I, Particle Interaction, ed. by W. H. Marlow (New York: Springer-Verlag, 1980), p. 117.

Marshall, J. R. et al., "Planetary Science," in Microgravity Particle Research on the Space Station, Report of a Workshop Held at NASA Ames Research Center 22-24 August 1985, ed. by S. W. Squyres et al. (Moffett Field, CA: NASA Ames Research Center), p. 9.

McKay, C. P. et al., "Space Station Gas-Grain Simulation Facility: Application to Exobiology," 1986 COSPAR meeting, to appear in Space Research.

McMurry, P. H. and Grosjean, D., "Gas and Aerosol Wall Losses in Teflon Film Smog Chambers", Environ. Sci. Technol., Vol. 19, No. 12, 1985, p. 1176.

McMurry, P. H. and Rader, D. J., "Aerosol Wall Losses in Electrically Charged Chambers," Aerosol Science and Technology, Vol. 4, 1985, p. 249.

NASA TM-89606, Life Sciences Space Station Planning Document: A Reference Payload for the Exobiology Research Facilities (Washington, D.C.: NASA Office of Space Science and Applications, 1987)

Naumann, R. J., and Elleman, D. D., "Containerless Processing Technology," in Materials Sciences in Space, A Contribution to the Scientific Basis of Space Processing, edited by B. Feuerbacher, H. Hamacher, and R. J. Naumann (New York: Springer-Verlag, 1986), p. 294.

Penner, S. S., Bernard, J. M. and Jerskey, T. "Laser Scattering from Moving Polydisperse Particles in a Flame II: Preliminary Experiments", Acta Astronautica, V. 3, p. 93, (1976).

Pluchino, A. B., "Radiometric Levitation of Spherical Carbon Aerosol Particles using a Nd: YAG Laser," Applied Optics, Vol. 22, No. 12, 15 June 1983, p. 1861.

Preining, O., "Photophoresis," in Aerosol Science, ed. by C. N. Davies (New York: Academic Press, 1966), p. 111.

Rhim, W. K. et al., "Development of an Electrostatic Positioner for Space Material Processing," Rev. Sci. Instrum., Vol. 56, No. 2, Feb. 1985, p. 307.

Roberts, J. H. and Webb, M. J., "Measurement of Droplet Size for Wide Range Particle Distributions," AIAA Journal, V. 2, pp. 583-585, (1964).

Robinson, D. M. and Chu, W. P., "Diffraction Analysis of Doppler Signal Characteristics for a Cross-Beam Laser Doppler Anemometer," Applied Optics, V. 14, p. 2177, (1975).

Rocke, M. J., Copper-Coated Laser-Fusion Targets Using Molecular-Beam Levitation, UCRL-86114 (Livermore, CA: Lawrence Livermore National Laboratory, September 8, 1981).

Rush, J. E. et al., "Properties of a Constricted-Tube Air-Flow Levitator," in Materials Processing in the Reduced Gravity Environment of Space, edited by G. E. Rindome (New York: Elsevier Science Publishing Co., Inc., 1982), also Appendix B in Containerless Processing Technology Analysis Final Report, 08 May 1980 - 31 Aug. 1982 (Huntsville, Alabama: University of Alabama, 1982).

Simmons, H. C., "The Correlation of Drop-size Distributions in Fuel Nozzle Sprays," J. of Engineering for Power, V. 99, pp. 309-314 (1977).

Spruch, L., "Retarded, or Casimir, Long-Range Potentials," Physics Today, Vol. 39, No. 11, Nov. 1986, p. 37.

Spurny, K. R., "Environmental and Biological Disperse System," in Physical and Chemical Characterization of Individual Airborne Particles, ed. by K. R. Spurny (New York: John Wiley & Sons, 1986), p. 16.

Straubel, E. and Straubel, H., "Electro-optical Measurement of Chemical and Physical Changes Taking Place in an Individual Aerosol Particle," in Physical and Chemical Characterization of Individual Airborne Particles, ed. by K. R. Spurny (New York: Halsted Press: a division of John Wiley and Sons, 1986), p. 127.

Swithenbank, J., Beer, J., Taylor, D. S., Abbot, D. and McCreath, C. G. "A Laser Diagnostic Technique for the Measurement of Droplet and Particle Size Distribution", in Experimental Diagnostics in Gas-Phase Combustion Systems, (B. T. Zinn, ed.) pp. 421-447, Progress in Astronautics and Aeronautics, V. 53, 1977.

Tiwary, R., "Acoustically Generated Turbulence and its Effect on Acoustic Agglomeration, "J. Acoust. Soc. Am., Vol. 76, No. 3, Sept. 1984, p. 841.

Thompson, B. J., J. Physics E., V. 7, pp. 781-788 (1974).

Trolinger, J. D., "Particle Field Diagnostics by Holography", AIAA Paper 80-0018, American Institute of Aeronautics and Astronautics, New York, 1980.

Twomey, S., Atmospheric Aerosols (New York: Elsevier Scientific Publishing Company, 1977).

Ungut, A., Yule, A. J., Taylor, D. S., and Chigier, N. A., "Simultaneous Velocity and Particle Size Measurements in Two Phase Flows by Laser Anemometry," AIAA Paper 78-74, AIAA 16th Aerospace Sciences Meeting, Huntsville, Alabama, January 10-18, 1978.

Wang, T. G., "Progress in Containerless Science and Technologies," in Manufacturing in Space presented at the Winter Annual Meeting of the American Society of Mechanical Engineers, Boston, Mass, Nov. 13-18, 1983, ed. by L. Kops (New York: The American Society of Mechanical Engineers, 1983), p. 77.

Wang, T. G., "Applications of Acoustics in Space." in Proceedings of the International School of Physics<<Enrico Fermi>>Course XCII, edited by D. Setle (New York: Elsevier Science Publishing Co., Inc., 1986), p. 294.

Weiss-Wrana, K., "Optical Properties of Interplanetary Dust: Comparison with Light Scattering by Larger Meteoritic and Terrestrial Grains," Astron. Astrophys., Vol. 126, 1983, p. 240.

Whymark, R. et al., "Acoustic Levitation Materials Processing Systems," AIAA Paper No. 79-0370, 17th Aerospace Sciences Meeting, New Orleans, LA, Jan. 15-17, 1979.

Yule, A. J., Chigier, N. A., Atakan, S. and Ungut, A., "Particle Size and Velocity Measurement by Laser Anemometry," AIAA Paper 77-214, 1977.

Zimon, A. D., Adhesion of Dust and Powder, 2nd ed., 1980, translated from Russian by R. K. Johnston (New York: Consultants Bureau, 1982).

APPENDIX A

SELF PRESERVING SOLUTION FOR COAGULATION OF FRACTAL PARTICLES

The following is a generalization of the derivation (Friedlander and Wang, 1966) for ordinary particles (constant total particle volume per system volume). The following assumes constant total particle mass per system volume. In the following, parts of sentences are borrowed without the use of quotations.

The kinetic equation for coagulation of particles is

$$\frac{\partial n \, (m,t)}{\partial t} = \frac{1}{2} \int_{o}^{m} \beta(\widetilde{m},m-\widetilde{m}) \, n(\widetilde{m},t) \, n(m-\widetilde{m},t) \, d\widetilde{m} \qquad (A-1)$$

$$- \int_{o}^{\infty} \beta(\widetilde{m},m) \, n(\widetilde{m},t) \, n(m,t) \, d\widetilde{m},$$

where
   m = mass of a particle (kg),

   t = time (s),

   n = number of particles per unit volume in the mass range m to m+dm ($kg^{-1} \, m^{-3}$), and

$\beta(\widetilde{m},m)$ = collision frequency factor between particles of mass $\widetilde{m}$ and m ($m^3/s$).

For coagulation by Brownian motion

$$\beta(m,\widetilde{m}) = \frac{2kT}{3\mu} \, [r(m) + r(\widetilde{m})] \, \left[\frac{1}{r(m)} + \frac{1}{r(\widetilde{m})}\right], \qquad (A-2)$$

where

   k = Boltzmann's constant ($1.38 \times 10^{-23}$ J/K),

   T = temperature (K),

   $\mu$ = fluid viscosity ($N-s/m^2$), and

   r = particle radius (m).

73

For a fractal particle

$$m \propto r^z,$$ 

(A-3)

where z is between 1.7 and 2.5.  Using (A-3) in (A-2) yields

$$\beta(m,\tilde{m}) = \frac{2kT}{3\mu} (m^{1/z} + \tilde{m}^{1/z})(m^{-1/z} + \tilde{m}^{-1/z}).$$

(A-4)

The total number of particles per unit volume N(t) and the total mass of particles per unit volume $\phi$, are given by

$$N(t) = \int_0^\infty n(m,t)\, dm, \text{ and}$$

(A-5)

$$\phi = \int_0^\infty m\, n(m,t)\, dm.$$

(A-6)

The following transformation is introduced:

$$n(m,t) = \frac{[N(t)]^2}{\phi} \Phi(\eta,\tau),$$

(A-7)

$$\eta = \frac{N(t)m}{\phi}, \text{ and}$$

(A-8)

$$\tau = \left[\frac{N(t)}{N(0)}\right]^2.$$

(A-9)

If $\beta(m,\tilde{m})$ is a homogeneous function of its arguments, substitution of (A-7) in (A-1) yields

$$\left[ \int_0^\infty \int_0^\infty \beta(\eta,\tilde{\eta}) \, \Phi(\eta,\tau) \, \Phi(\tilde{\eta},\tau) \, d\eta \, d\tilde{\eta} \right]$$

$$\bullet \left[ \eta \frac{\partial \, \Phi(\eta,\tau)}{\partial \eta} + 2 \, \Phi(\eta,\tau) + 2\tau \frac{\partial \, \Phi(\eta,\tau)}{\partial \tau} \right]$$

$$+ \int_0^\eta \beta(\tilde{\eta},\eta-\tilde{\eta}) \, \Phi(\tilde{\eta},\tau) \, \Phi(\eta-\tilde{\eta},\tau) \, d\tilde{\eta}$$

$$-2 \int_0^\infty \beta(\eta,\tilde{\eta}) \, \Phi(\tilde{\eta},\tau) \, \Phi(\eta,\tau) \, d\tilde{\eta} = 0 \, . \tag{A-10}$$

Using (A-7) in (A-5) and (A-6) yields

$$\int_0^\infty \Phi(\eta,\tau) \, d\eta = 1 \text{ and} \tag{A-11}$$

$$\int_0^\infty \eta \, \Phi(\eta,\tau) \, d\eta = 1 \, . \tag{A-12}$$

Letting $\qquad 2\tau \dfrac{\partial \, \Phi(\eta,\tau)}{\partial \tau} = 0 \qquad$ (Friedlander and Wang, 1966)

and using (A-4) in (A-10) yields

$$(1 + ab) \, \eta \frac{d\psi(\eta)}{d\eta} + (2ab - b\eta^{1/z} - a\eta^{-1/z}) \, \psi(\eta) \tag{A-13}$$

$$+ \int_0^\eta \psi(\tilde{\eta}) \, \psi(\eta - \tilde{\eta}) \left[ 1 + \left( \frac{\eta - \tilde{\eta}}{\tilde{\eta}} \right)^{1/z} \right] d\tilde{\eta} = 0 \, ,$$

75

where

$\psi(\eta)$ = replacement for $\hat{}(\eta, \tau)$ , which is assumed to be independent of $\tau$ ,

$$a = \int_o^\infty \eta^{1/z} \psi(\eta) \, d\eta, \text{ and} \qquad \text{(A-14)}$$

$$b = \int_o^\infty \eta^{-1/z} \psi(\eta) \, d\eta. \qquad \text{(A-15)}$$

Letting

$$\psi(\eta) = \frac{(1 + ab)^{z+1}}{a^z} \chi(\zeta) \quad \text{and} \qquad \text{(A-16)}$$

$$\eta = \frac{a^z}{(1 + ab)^z} \zeta \, , \qquad \text{(A-17)}$$

(A-13) becomes

$$\zeta \frac{d\chi(\zeta)}{d\zeta} + [2\alpha - \alpha(1 - \alpha)\zeta^{1/z} - \zeta^{-1/z}] \chi(\zeta) \qquad \text{(A-18)}$$

$$+ \int_o^\zeta \chi(\tilde{\zeta}) \chi(\zeta - \tilde{\zeta}) \left[ 1 + \left( \frac{\zeta - \tilde{\zeta}}{\tilde{\zeta}} \right)^{1/z} \right] d\tilde{\zeta} = 0,$$

where

$$\alpha = \frac{ab}{(1 + ab)} \, . \qquad \text{(A-19)}$$

In terms of $\chi(\zeta)$, Eqs. (A–11), (A–12), (A–14), and (A–15) become

$$\int_{o}^{\infty} \chi(\zeta)\, d\zeta = 1 - \alpha,$$ 
(A-20)

$$\int_{o}^{\infty} \zeta \chi(\zeta)\, d\zeta = \frac{1}{a^{z}\,(1 - \alpha)^{z-1}},$$ 
(A-21)

$$\int_{o}^{\infty} \zeta^{1/z} \chi(\zeta)\, d\zeta = 1, \text{ and}$$ 
(A-22)

$$\int_{o}^{\infty} \zeta^{-1/z} \chi(\zeta)\, d\zeta = \alpha(1 - \alpha)$$ 
(A-23)

For the lower end of the spectrum, the integral term in (A–18) may be neglected:

$$\zeta\, \frac{d\,\chi(\zeta)}{d\zeta} + [2\alpha - \alpha(1 - \alpha)\,\zeta^{1/z} - \zeta^{-1/z}]\, \chi(\zeta) = 0,$$ 
(A-24)

a solution to which is

$$\chi(\zeta) = \frac{C_{1}}{\zeta^{2\alpha}}\, \exp\,[z\,\alpha(1 - \alpha)\,\zeta^{1/z} - z\,\zeta^{-1/z}],$$ 
(A-25)

where $C_{1}$, is an integration constant. For the upper end of the spectrum, the second term in (A–18) is negligible:

$$\zeta\, \frac{d\chi(\zeta)}{d\zeta} + \int_{o}^{\zeta} \chi(\tilde{\zeta})\, \chi(\zeta - \tilde{\zeta})\left[ 1 + \left(\frac{\zeta - \tilde{\zeta}}{\tilde{\zeta}}\right)^{1/z} \right] d\tilde{\zeta} = 0,$$ 
(A-26)

A solution to which is

$$\chi(\zeta) = \frac{C_2 \, e^{-C_2 \zeta}}{1 + B \, (1 - 1/z, \; 1 + 1/z)} \, , \qquad \text{(A-27)}$$

Where $C_2$, is an integration constant and B is the beta function. Using the substitutions

$$\zeta = e^x, \text{ and} \qquad \text{(A-28)}$$
$$y(x) = \chi(\zeta), \qquad \text{(A-29)}$$

Eq. (A-18) may be written as

$$\frac{dy(x)}{dx} + [2\alpha - \alpha(1 - \alpha)e^{x/z} - e^{-x/z}] \, y(x)$$

$$+ \int_{-\infty}^{x} y(\widetilde{x}) \, y[\ln(e^x - e^{\widetilde{x}})]$$

$$\cdot \left[ 1 + \left( \frac{e^x - e^{\widetilde{x}}}{e^{\widetilde{x}}} \right)^{1/z} \right] e^{\widetilde{x}} \, d\widetilde{x} = 0 \, . \qquad \text{(A-30)}$$

Using the substitution

$$t = \frac{2}{z} \, (x - \widetilde{x}) \, , \qquad \text{(A-31)}$$

the integral in (A-30) may be written as

$$\frac{z}{2} \, e^x \int_{0}^{\infty} y(x - \frac{z}{2} t) \, y[x + \ln(1 - e^{-\frac{z}{2} t})] \, [e^{-\frac{t}{2}} + (1 - e^{-\frac{zt}{2}})^{1/z}]$$

$$\cdot e^{\frac{(1 - z)}{2} t} \, dt. \qquad \text{(A-32)}$$

Eq. (A-30) was solved for z=2 ($m \propto r^2$) over the range in which $y(x)$ is significant: $-4.4 \leq x \leq 6.0.$ The starting value $y(-4.4)$ was given by (A-25) with $C_1$ and $\alpha$ guessed until Eqs. (A-20), (A-22), and (A-23) were satisfied. Then $C_2$ was chosen to match the upper end solution. Using crude stepwise integration (see Table A-1) on a very slow desk top computer yielded the following very approximate values:

$C_1 = 0.4$

$\alpha = 0.6$

$a = 0.90$

$b = 0.42$

$C_2 = 0.2$

The fit for the upper end solution was very poor and the correct value of $C_2$ may be an order of magnitude higher or lower than 0.2. However, this value of $C_2$ is sufficiently accurate to give order of magnitude times for formation of large particles.

The time to form a unit density of particles larger than mass $m_1$, will now be computed. Using the above values of a, b, and $C_2$ in (A-16), (A-17), and (A-27) yields

$$\psi(\eta) = 0.25 \ e^{-0.47\eta}. \tag{A-33}$$

Using (A-7), (A-8), and (A-33) yields

$$n(m,t) = \frac{[N(t)]^2}{\phi} \ 0.25 \ \exp\left[-0.47 \ \frac{N(t)m}{\phi}\right]. \tag{A-34}$$

At time t, the density of particles with mass greater than $m_1$, is

$$N_1(t) = \int_{m_1}^{\infty} n(m,t) \ dm = 0.54 \ N(t) \ \exp\left[-0.47 \ \frac{N(t) \ m_1}{\phi}\right]. \tag{A-35}$$

*Table A-1 Program for Solution of Equations A-30 Thru A-32*

```
1   ! Coag5
5   DIM Y(1000)
10  Z=2
20  Alfa=.60
30  C1=.4
40  Xmax=5.4
50  Xmin=-4.4
60  Nx=400
70  Dx=(Xmax-Xmin)/Nx
75  Dt=2/Z*Dx
80  Zeta1=EXP(Xmin)
90  Exp1=EXP(Z*Alfa*(1-Alfa)*Zeta1^(1/Z)-Z*Zeta1^(-1/Z))
100 Y(1)=C1/Zeta1^(2*Alfa)*Exp1
105 I=0
110 X=Xmin-Dx
120 X=X+Dx
130 I=I+1
140 Term1=(2*Alfa-Alfa*(1-Alfa)*EXP(X/Z)-EXP(-X/Z))*Y(I)
145 Sum=0
147 IF X=Xmin THEN GOTO 250
150 Tmax=(X-Xmin)*2/Z
160 Tmin=-(2/Z)*LOG(1-EXP(Xmin-X))
165 IF Tmin>Tmax-Dt THEN GOTO 250
170 T=Tmin-Dt
190 T=T+Dt
200 I1=INT((X-Z/2*T-Xmin)/Dx+1.1)
210 I2=INT((X+LOG(1-EXP(-(Z/2)*T))-Xmin)/Dx+1.1)
220 Term2=EXP(-T/2)+(1-EXP(-Z*T/2))^(1/Z)
230 Sum=Sum+Y(I1)*Y(I2)*Term2*EXP((1-Z)*T/2)
240 IF T<Tmax-1.1*Dt THEN GOTO 190
250 Y(I+1)=Y(I)-Dx*(Term1+Dt*(Z/2)*EXP(X)*Sum)
260 PRINT " X=";X+Dx," Y=";Y(I+1)
270 IF X<Xmax-1.1*Dx THEN GOTO 120
280 Sum1=0
290 Sum2=0
300 Sum3=0
310 Sum4=0
315 X=Xmin-Dx
320 FOR I=1 TO Nx
330     X=X+Dx
340     Zeta=EXP(X)
350     Dzeta=Zeta*Dx
360     Sum1=Sum1+Y(I)*Dzeta
370     Sum2=Sum2+Zeta*Y(I)*Dzeta
380     Sum3=Sum3+Zeta^(1/Z)*Y(I)*Dzeta
390     Sum4=Sum4+Zeta^(-1/Z)*Y(I)*Dzeta
400 NEXT I
410 PRINT " Input C1 = ";C1
420 PRINT " Input Alfa = ";Alfa
430 K1=Sum1
440 K2=Sum2
450 K3=Sum3
460 K4=Sum4
470 PRINT " K1 = ";K1
480 PRINT " K2 = ";K2
490 PRINT " K3 = ";K3
500 PRINT " K4 = ";K4
510 Ck1=1-Alfa
520 Ck4=Alfa*(1-Alfa)
530 PRINT " 1 - Alfa = ";Ck1
540 PRINT " Alfa*(1-Alfa) = ";Ck4
610 STOP
620 END
```

The total density of particles is (Ludlam, 1980)

$$N(t) = \frac{1}{1/N_o + Kt},$$ (A-36)

where

$N_o = N(0)$, and

$K \approx 5 \times 10^{-10} \text{ cm}^3/\text{s} = 5 \times 10^{-16} \text{ m}^3/\text{s}.$

Since $N_0 > 10^8/\text{cm}^3 = 10^{14}/\text{m}^3$ and $t > 1$ hour (for the cases to be considered),

$$N(t) \approx (Kt)^{-1}.$$ (A-37)

The mass $m_1$, is given by

$$m_1 = m_o \left(\frac{r_1}{r_o}\right)^2,$$ (A-38)

while the total mass density is

$$\phi = N_o m_o.$$ (A-39)

Using (A-37) through (A-39) in (A-35) yields

$$N_1(t) = \frac{0.54}{Kt} \exp\left[\frac{-0.47}{Kt N_o} \left(\frac{r_1}{r_o}\right)^2\right].$$ (A-40)

Setting $N_1(t) = 1/V$ where $V = 0.01 \text{ m}^3 = (8.5 \text{ inches})^3$ = useable volume and using $r_0 = 30 \text{ nm} = 3 \times 10^{-8}$ m and $r_1 = 1 \text{ mm} = 10^{-3}$ m yields the second column of Table A-2. The particle volume fraction is

$$f_{vol}(t) = \int_o^\infty v\, n(m,t)\, dm = 9.2\, r_o^3\, (Kt)^{\frac{1}{2}}\, N_o^{3/2},$$ (A-41)

and this is listed in the third column of Table A-2 corresponding to the times of the second column. It is apparent from Table A-2 that for initial number density less than $10^{11}/\text{cm}^3$ the time is unreasonably long, while for the initial number density greater than $10^{12}/\text{cm}^3$ the final volume of particles exceeds the system volume. For an initial density of 2.75 g/cm$^3$, for a particle of initial radius 30 nm, a particle of final radius 1 mm will have a final density of $8.25 \times 10^{-5}$ g/cm$^3$. Using this density and a chamber radius of

Table A-2 Time to Create One Particle Per 0.01 $m^3$ with Radius Greater than 1 mm.

| Initial Density ($cm^{-2}$) | Time | Final Volume Fraction |
|---|---|---|
| $10^8$ | 35 years | $1.8 \times 10^{-4}$ |
| $10^9$ | 2.7 years | $1.6 \times 10^{-3}$ |
| $10^{10}$ | 81 days | $1.5 \times 10^{-2}$ |
| $10^{11}$ | 7 days | 0.14 |
| $10^{12}$ | 14 hours | 1.2 |
| $10^{13}$ | 1.3 hours | 12 |
| $10^{14}$ | 7 minutes | 114 |

Conditions:
    initial radius = 30 nm
    gas: standard atmosphere

0.5 m, Eq. 2.3-3 yields a time of 57 days for a 1 mm radius particle to reach the wall due to a gravitational acceleration of $10^{-5}$ g. Therefore, residual gravity is not a problem. Also, from Table 2.3-1 it is apparent that Brownian motion is not a problem even for the initial particles.

COMPARISON OF ELECTROSTATIC LEVITATION OF A PARTICLE HAVING A NET
CHARGE WITH THAT OF A DIELECTRIC PARTICLE HAVING NO NET CHARGE

A dielectric particle with no net charge will be levitated in the field
of a spherical conductor of radius $r_{inner}$. An outer sphere (not
necessarily conducting) of radius $r_{outer}$ will serve as the outer wall
of the chamber. The center of the dielectric particle will be at
$r_{mid}$:

$$r_{mid} = \frac{r_{inner} + r_{outer}}{2} .$$  (B-1)

The particle is a cube with side $\Delta r$ , positioned such that the
normal to one side is in the radial direction. An electric field
normal to a thin planar dieletric induces a surface charge per unit
area $q_1/A$ on one face and a surface charge per unit area $-q_1/A$ on
the other face such that (Halliday and Resnick, 1962)

$$D = \varepsilon_o E + \frac{q_1}{A} ,$$  (B-2)

where

   $D$ = electric displacement based only on free charges (neglecting
   $q_1$) $(C/m^2)$,

   $\varepsilon_o$ = permittivity of free space $(8.854 \times 10^{-12}\ F/m)$, and

   $E$ = electric field strength $(V/m)$.

For an isotropic media (Halliday and Resnick, 1962)

$$D = \kappa \varepsilon_o E,$$  (B-3)

where $\kappa$ is the dielectric constant and is equal to unity for a vacuum.
Using (B-3) in (B-2) yields

$$\frac{q_1}{A} = D \left( 1 - \frac{1}{\kappa} \right) .$$  (B-4)

Eq. (B-4) has been derived for an infinite planar slab of dielectric. The crude approximation is now made that Eq. (B-4) applies to the cubic particle:

$$\frac{q_1}{(\Delta r)^2} = D_{mid} \left( 1 - \frac{1}{K} \right), \text{ and}$$

$$q_1 = (\Delta r)^2 D_{mid} \left( 1 - \frac{1}{K} \right),$$

(B-5)

where $D_{mid}$ is D evaluated at $r_{mid}$. Since for a positive potential on the inner sphere the inner surface of the particle has a charge $-q_1 < 0$ and the outer surface has a charge $q_1 > 0$, the net force on the particle is

$$F_E = -q_1 E(r_{mid} - \Delta r/2) + q_1 E(r_{mid} + \Delta r/2).$$

(B-6)

It will be assumed that each charge resides just inside the surface of the particle such that

$$E(r_{mid} - \Delta r/2) = \frac{D(r_{mid} - \Delta r/2)}{K \varepsilon_o} = \frac{q}{4\pi K \varepsilon_o (r_{mid} - \Delta r/2)^2},$$

(B-7)

$$E(r_{mid} + \Delta r/2) = \frac{D(r_{mid} + \Delta r/2)}{K \varepsilon_o} = \frac{q}{4\pi K \varepsilon_o (r_{mid} + \Delta r/2)^2},$$

(B-8)

where $K \neq 1$ and q is the charge on the spherical conductor. Also

$$D_{mid} = \frac{q}{4\pi r_{mid}^2}, \text{ and}$$

(B-9)

$$q = 4\pi \varepsilon_o r_{inner} V_{inner},$$

(B-10)

where $V_{inner}$ is the voltage on the spherical conductor. Using (B-5), (B-7), (B-8), (B-9), and (B-10) in (B-6) yields

$$F_E = -\frac{\varepsilon_o \, (K - 1) \, r_{inner}^2 \, V_{inner}^2 \, (\Delta r)^2}{K^2 \, r_{mid}^2} \left[\frac{1}{(r_{mid} - \Delta r/2)^2} - \frac{1}{(r_{mid} + \Delta r/2)^2}\right] . \qquad \text{(B-11)}$$

The term in brackets in (B-11) is approximately equal to $2 \, \Delta r / r_{mid}^3$ such that

$$F_E = -\frac{2 \, \varepsilon_o \, (K - 1) \, r_{inner}^2 \, V_{inner}^2 \, (\Delta r)^3}{K^2 \, r_{mid}^5} . \qquad \text{(B-12)}$$

It will be assumed that an acceleration of magnitude $10^{-5}g$ is directed radially inward:

$$F_g = - (\Delta r)^3 \, \rho \, 10^{-5}g, \qquad \text{(B-13)}$$

where $\rho$ is the density of the particle. Equating (B-12) and (B-13) yields

$$V_{inner} = \frac{K}{r_{inner}} \sqrt{\frac{r_{mid}^5 \, \rho \, 10^{-5}g}{2(K - 1) \, \varepsilon_o}} . \qquad \text{(B-14)}$$

A typical dielectric constant is that of quartz (E perpendicular to optic axis):

$$K = 4.34.$$

Using a density of

$$\rho = 1 \ g/cm^3 \ (\text{not that of quartz})$$

and radii of

$$r_{inner} = 10 \ cm,$$

$$r_{outer} = 20 \ cm, \ and$$

$$r_{mid} = 15 \ cm,$$

yields $V_{inner} = 1.54 \times 10^4$ volts. It may be noted that the size of the particle does not enter into Eq. (B-14).

To levitate a spherical particle charged with $n_e$ electrons in the arrangement described above requires that

$$n_e \ V_{inner} = \frac{r_{mid}^2 \ \frac{4}{3} \pi R_p^3 \ \rho \ 10^{-5}g}{r_{inner} \ e} \ , \tag{B-15}$$

where $R_p$ is the radius of the particle. Eq. (B-15) is evaluated in Table B-1.

Table B-1 Conditions for Levitation of a Charged Particle

| Particle Radius ($\mu$) | Number of electrons times voltage (V) on inner spherical wall |
|---|---|
| 1 | 0.577 |
| 10 | 577 |
| 100 | $5.77 \times 10^5$ |
| 1000 | $5.77 \times 10^8$ |

Conditions:

  Radius of inner wall = 10 cm
  Radial position of particle = 15 cm from center
  Density of particle = 1 g/cm$^3$
  Residual gravity = $10^{-5}$ g

Levitation at $10^{-5}$g via the dielectric effect is probably not practical because it requires a voltage on the inner wall of 1.54 x $10^4$ volts. On the other hand, levitating a particle of radius 1 μm charged with one electron (With the electron at the center of the particle, the surface voltage would be $1.44 \times 10^{-3}$ V.) requires a voltage on the inner wall of only 0.577 volts. Also, levitating a particle of radius 1 mm charged to a surface voltage of 10 volts, requires a voltage on the inner wall of only 83.3 volts.

## AMPLITUDE OF MOTION DUE TO BROWNIAN MOTION
## WITHIN AN ACOUSTIC POTENTIAL WELL

For a one dimensional standing wave the acoustic radiation pressure force is given by (see Eq. 2.9-2)

$$F = K \sin 2kx, \tag{C-1}$$

where

$$K = \frac{5\pi}{6} \frac{p_1^2}{\rho c^2} k a^3. \tag{C-2}$$

Since only an order of magnitude answer is desired, Eq. (C-1) will be applied to a spherical potential well, with x being the radial coordinate and x=o being the center of the well. The translational energy of a particle due to Brownian motion in a gas is

$$E = \frac{3}{2} k_B T, \tag{C-3}$$

where $k_B$ is Boltzmann's constant ($1.38 \times 10^{-23}$ J/K). Therefore the amplitude of the motion $\Delta x$ satisfies

$$\frac{3}{2} k_B T = \int_o^{\Delta x} F \, dx'. \tag{C-4}$$

Using (C-1) in (C-4), integrating and then using the approximation

$$\cos z = 1 - \frac{z^2}{2} \tag{C-5}$$

yields

$$\Delta x = \sqrt{\frac{3 k_B T}{2 K k}} . \tag{C-6}$$

As a check, an approximation to this result will be derived by equating the time for diffusing from the center of the well to $\Delta x$ to the time for the force F to return the particle from $\Delta x$ to the center of the well. From Eq. (2.3-1) the time to diffuse to $\Delta x$ is

$$t = \frac{(\Delta x)^2}{2k_B TB} . \tag{C-7}$$

The time for the force F to return the particle from $\Delta x$ to the center of the well is

$$t = \frac{\Delta x}{\bar{v}} , \tag{C-8}$$

where

$$\bar{v} = \bar{F} B, \tag{C-9}$$

$$\bar{F} \approx K \sin 2k \frac{\Delta x}{2} = K \sin k\Delta x \approx K \, k\Delta x. \tag{C-10}$$

Using (C-7) thru (C-10) yields

$$\Delta x = \sqrt{\frac{2 k_B T}{K k}} , \tag{C-11}$$

which is greater than (C-6) by a factor of only $\sqrt{2}/\sqrt{3/2} = \sqrt{4/3}$ = 1.15, which implies an error of only 15%. Balancing the maximum value of the force (when 2kx = $\pi/2$) against an acceleration of $10^{-5}$g yields

$$K = \frac{4}{3} \pi a^3 \rho_p \, 10^{-5}g, \tag{C-12}$$

where $\rho_p$ is the mass density of the particle. The wavenumber is given by

$$k = \frac{2\pi}{\lambda} = \frac{2\pi f}{c} , \tag{C-13}$$

C-2

91

where

f = frequency (Hz),

c = speed of sound (m/s),

$$c = \sqrt{\frac{\gamma \, k_B T}{m}} ,$$
(C-14)

$\gamma$ = ratio of specific heats (1.40 for diatomic gases), and

m = mass of gas molecule (kg).

Using (C-12) and (C-13) in (C-6) yields

$$\Delta x = \sqrt{\frac{9 \, k_B T \, c}{16 \pi^2 \, a^3 \, \rho_p \, 10^{-5} g \, f}} .$$
(C-15)

Therefore the largest $\Delta x$ is produced by the smallest particle radius a. M. Barmatz of JPL (private communication via G. Fogleman of RCA, July, 1987) has estimated that streaming limits the minimum particle radius to 1% of the wavelength:

a = 0.01 $\lambda$, and

a = 0.01 c/f.
(C-16)

Using (C-14) thru (C-16) yields

$$\Delta x = \frac{750}{\pi} \sqrt{\frac{m}{\gamma \, \rho_p \, 10^{-5} g}} \, f.$$
(C-17)

For nitrogen gas:

$\gamma$ = 1.40, and
m = 4.65x10$^{-26}$ kg.
For
$\rho_p$ = 1 g/cm$^3$,
$\Delta x$ = 1.39x10$^{-10}$ f.
(C-18)

Equations (C-16) and (C-18) are evaluated in Table C-1, from which it is evident that for practical frequencies (<< MHz) the amplitude is less than the radius of the particle. Therefore acoustic levitation in residual gravity prevents Brownian motion.

Table C-1 Amplitude of Brownian Motian in an Acoustic Potential Well

| f (Hz) | a(m) | $\Delta x$ (m) | $\Delta x/a$ |
|---|---|---|---|
| $10^3$ | $3.53 \times 10^{-3}$ | $1.39 \times 10^{-7}$ | $3.94 \times 10^{-5}$ |
| $10^4$ | $3.53 \times 10^{-4}$ | $1.39 \times 10^{-6}$ | $3.94 \times 10^{-3}$ |
| $10^5$ | $3.53 \times 10^{-5}$ | $1.39 \times 10^{-5}$ | $3.94 \times 10^{-1}$ |
| $10^6$ | $3.53 \times 10^{-6}$ | $1.39 \times 10^{-4}$ | $3.94 \times 10^{1}$ |

| NASA National Aeronautics and Space Administration | Report Documentation Page | | |
|---|---|---|---|

| 1. Report No. CR-177468 | 2. Government Accession No. | 3. Recipient's Catalog No. |
|---|---|---|
| 4. Title and Subtitle Feasibility Study for Gas-Grain Simulation Facility | | 5. Report Date September 1987 |
| | | 6. Performing Organization Code |
| 7. Author(s) J. B. Miller and B. C. Clark | | 8. Performing Organization Report No. |
| | | 10. Work Unit No. 805-19 |
| 9. Performing Organization Name and Address Martin Marietta Astronautics Group P.O. Box 179 Denver, CO 80201 | | 11. Contract or Grant No. NAS 2-11370 |
| | | 13. Type of Report and Period Covered Contractor Report Final |
| 12. Sponsoring Agency Name and Address Solar System Exploration Branch NASA-Ames Research Center Moffett Field, CA 94035 | | 14. Sponsoring Agency Code SLS |

15. Supplementary Notes

Point of contact:  John Billingham  
415-694-5181

Life Science Division  
NASA Ames Research Center MS 239-11  
Moffett Field, CA  94035

16. Abstract

This report presents the results of a feasibility study conducted to examine physical phenomena involved in gas-grain interactions using a Gas-Grain Simulation Facility (GGSF).

| 17. Key Words (Suggested by Author(s)) Gas-Grain Microgravity Space Station GGSF | 18. Distribution Statement Unlimited Subject Category 070 | | |
|---|---|---|---|

| 19. Security Classif. (of this report) Unclassified | 20. Security Classif. (of this page) Unclassified | 21. No. of pages 111 | 22. Price |
|---|---|---|---|

NASA FORM 1626 OCT 86

# PREPARATION OF THE REPORT DOCUMENTATION PAGE

The last page of a report facing the third cover is the Report Documentation Page, RDP. Information presented on this page is used in announcing and cataloging reports as well as preparing the cover and title page. Thus it is important that the information be correct. Instructions for filling in each block of the form are as follows:

Block 1. Report No. NASA report series number, if preassigned.

Block 2. Government Accession No. Leave blank.

Block 3. Recipient's Catalog No. Reserved for use by each report recipient.

Block 4. Title and Subtitle. Typed in caps and lower case with dash or period separating subtitle from title.

Block 5. Report Date. Approximate month and year the report will be published.

Block 6. Performing Organization Code. Leave blank.

Block 7. Author(s). Provide full names exactly as they are to appear on the title page. If applicable, the word editor should follow a name.

Block 8. Performing Organization Report No. NASA installation report control number and, if desired, the non-NASA performing organization report control number.

Block 9. Performing Organization Name and Address. Provide affiliation (NASA program office, NASA installation, or contractor name) of authors.

Block 10. Work Unit No. Provide Research and Technology Objectives and Plans (RTOP) number.

Block 11. Contract or Grant No. Provide when applicable.

Block 12. Sponsoring Agency Name and Address. National Aeronautics and Space Administration, Washington, D.C. 20546-0001. If contractor report, add NASA installation or HQ program office.

Block 13. Type of Report and Period Covered. NASA formal report series; for Contractor Report also list type (interim, final) and period covered when applicable.

Block 14. Sponsoring Agency Code. Leave blank.

Block 15. Supplementary Notes. Information not included elsewhere: affiliation of authors if additional space is required for block 9, notice of work sponsored by another agency, monitor of contract, information about supplements (film, data tapes, etc.), meeting site and date for presented papers, journal to which an article has been submitted, note of a report made from a thesis, appendix by author other than shown in block 7.

Block 16. Abstract. The abstract should be informative rather than descriptive and should state the objectives of the investigation, the methods employed (e.g., simulation, experiment, or remote sensing), the results obtained, and the conclusions reached.

Block 17. Key Words. Identifying words or phrases to be used in cataloging the report.

Block 18. Distribution Statement. Indicate whether report is available to public or not. If not to be controlled, use "Unclassified-Unlimited." If controlled availability is required, list the category approved on the Document Availability Authorization Form (see NHB 2200.2, Form FF427). Also specify subject category (see "Table of Contents" in a current issue of STAR), in which report is to be distributed.

Block 19. Security Classification (of this report). Self-explanatory.

Block 20. Security Classification (of this page). Self-explanatory.

Block 21. No. of Pages. Count front matter pages beginning with iii, text pages including internal blank pages, and the RDP, but not the title page or the back of the title page.

Block 22. Price Code. If block 18 shows "Unclassified-Unlimited," provide the NTIS price code (see "NTIS Price Schedules" in a current issue of STAR) and at the bottom of the form add either "For sale by the National Technical Information Service, Springfield, VA 22161-2171" or "For sale by the Superintendent of Documents, U.S. Government Printing Office, Washington, DC 20402-0001," whichever is appropriate.